# Chapter 1

# Introduction

Chaotic systems have been a focal point of renewed interest for many researchers in the past few decades. Such nonlinear systems can occur in various natural and man-made systems, and are known to have great sensitivity to initial conditions [1].

Besides the theoretical interest in the analysis of such nonlinear systems, there is another dimension to that interest; namely, utilizing such systems for useful practical applications [2-13]. Many researchers have devoted themselves to finding new ways to control chaos more efficiently [14-17]. Chaotic phenomena are quite useful in many applications such as fluid mixing [18], human brain dynamics [19], and heart beat regulation [20], information processing, etc. Therefore, making a periodic dynamical system chaotic, or preserving chaos of a chaotic dynamical system, is very meaningful and worthy to be investigated [21,22].

Fractional calculus is a 300-year-old mathematical topic [23-26]. Although it has a long history, for many years it was not used in physics and engineering. However, during the last 10 years or so, fractional calculus starts to attract increasing attention of physicists and engineers from an application point of view [27,28]. It was found that many systems in interdisciplinary fields can be elegantly described with the help of fractional derivatives. Many systems are known to display fractional-order dynamics, such as viscoelastic systems [29], dielectric polarization [30], electrode–electrolyte polarization [31], electromagnetic waves [32], quantitative finance [33], and quantum evolution of complex systems [34].

There are few investigations about delay system with fractional order. In this proposal, chaos in new integral and fractional order double Ikeda delay systems is studied. A double Ikeda delay system consists of two traditional Ikeda delay systems which are coupled together. Numerical simulations display the chaotic behaviors of the integral and fractional order delay systems by phase portraits, Poincaré maps and bifurcation diagrams.

Since the pioneering work was given by Pecorra and Carroll [35], chaos synchronization [36-41] has become an important topic in engineering science. Many effective control schemes have been developed in a variety of fields, such as parameters adaptive control [42-49], observer-based control [50, 51], variable structure control [52, 53], active control [54-58], anti-control [59-63], nonlinear control [64-66] and so on. The applications of chaos synchronization are implemented extensively in secure communications, chemical, physical, and biological systems and neural networks.

Recently, the concept of synchronization has been extended the scope to, such as generalized synchronization, lag and anticipated synchronization, phase synchronization and anti-synchronization. The basic synchronization called complete synchronization is that the state vectors of the first system $x(t)$ is equal to the state vectors of the second system $y(t)$: $y(t) = x(t)$. The lag synchronization [67] is that the state vector of the second system $y$ delays that of driver system $x$: $y(t) = x(t-T)$ with positive $T$. If $T$ is negative, we have anticipated synchronization. Lag anti-synchronization [68] means $y(t) = -x(t-T)$. When $T$ is negative, we have anticipated anti-synchronization.

Time-delayed systems are ubiquitous in nature, technology, and society because of finite signal transmission times, switching speeds, and memory effects [69]. Therefore the study of chaos synchronization in these systems is of considerable practical significance. It is well known that dissipative systems with a nonlinear time-delayed feedback or ‘‘memory’’ can produce chaotic dynamics, and the dimension of their chaotic attractors can be made arbitrarily large by increasing their delay time sufficiently. Thus time-delay systems are good candidates for secure communications based on chaos synchronization [70].

This thesis is organized as follows. Chapter 2 gives the dynamic equation of double Ikeda system. The fractional derivative and its approximation are introduced. The system under study is described both in its integer and fractional forms. Numerical simulation results are presented.

In Chapter 3, it is discovered that lag synchronization and lag anti-synchronization appear for two identical double Ikeda systems, without any control scheme or coupling terms, but with different initial conditions.

In Chapter 4, the chaotic behaviors of double Ikeda systems are obtained by replacing the original constant delay time by a function of chaotic state variable of a second chaotic double Ikeda system. Numerical simulations are illustrated by phase portraits. Phase portrait is expressed by numerical analysis.

In Chapter 5, the chaotic behaviors of double Ikeda systems are obtained by replacing the parameters by different chaotic state variables of a third chaotic double Ikeda system. The method is named parameter excited method for synchronization which will be successfully used for uncoupled synchronization. Numerical simulations are illustrated by phase portraits and time histories.

In Chapter 6, conclusions are drawn.

# Chapter 2

# Chaos in Integral and Fractional Order Double Ikeda Systems

## 2.1 Preliminaries

In this Chapter, the chaotic behaviors in integral and fractional order double Ikeda systems are studied numerically by phase portraits, Poincaré maps and bifurcation diagrams. It is found that chaos exists for all systems with total orders of derivatives from 2 to 0.2.

## 2.2 Fractional Derivative and Its Approximation

The idea of fractional integrals and derivatives has been known since the development of the regular calculus, with the first reference probably being associated with Leibniz in 1695 [71].

Two commonly used definitions for the general fractional differintegral are the Grunwald definition and the Riemann-Liouville definition. The latter is given here

$$\frac{d^q f(t)}{dt^q} = \frac{1}{\Gamma(n-q)} \frac{d^n}{dt^n} \int_0^t \frac{f(\tau)}{(t-\tau)^{q-n+1}} d\tau \qquad (2.1)$$

where $n-1 \le q < n$ and $\Gamma(\cdot)$ is an Euler's gamma function.

The Laplace transformation of the Riemann-Liouville fractional derivative (2.1) is

$$L\left\{\frac{d^q f(t)}{dt^q}\right\} = s^q L\{f(t)\} - \sum_{k=0}^{n-1} s^k \left[\frac{d^{q-1-k} f(t)}{dt^{q-1-k}}\right]_{t=0}, \text{ for } n-1 \le q < n \qquad (2.2)$$

By considering the initial conditions to be zero, this formula reduces to the more expected and comforting form

$$L\left\{\frac{d^q f(t)}{dt^q}\right\} = s^q L\{f(t)\} \tag{2.3}$$

and the fractional integral of order q can be described as $F(s) = \frac{1}{s^q}$ in the frequency domain.

The standard definitions of the fractional differintegral do not allow direct implementation of the operator in time domain simulations of complicated systems with fractional elements. Using the standard integer order operators to approximate the fractional operators is an effective method to analyze such systems.

The approximation approach taken here is to approximate the system behavior in the frequency domain [72]. By utilizing frequency domain techniques based in Bode diagrams, one can obtain a linear approximation of a fractional order integrator. Thus an approximation of any desired accuracy over any frequency band can be achieved. Table I of Ref. [73] gives approximations for $\frac{1}{s^q}$ with $q = 0.1 \sim 0.9$ in steps of 0.1 with errors of approximately 2 dB from $\omega = 10^{-2}$ to $10^2$ rad/s. These approximations will be used in the following numerical simulations.

## 2.3 Integral and Fractional Order Double Ikeda Systems

The traditional Ikeda system is

$$\dot{x} = -ax - b \sin x_\tau \tag{2.4}$$

where $x_\tau \equiv x(t-\tau)$ with positive $\tau$. x is the phase lag of the electric field across the resonator, and $x(t-\tau)$ is the round trip time of the light in the resonator or feedback delay time in the coupled systems.

In this paper, we consider a new delay system which consists of two coupled Ikeda systems, called double Ikeda system:

$$\begin{cases} \dot{x} = -a_1 x - b_1 \sin x_{\tau_1} - c \sin y \\ \dot{y} = -a_2 y - b_2 \sin y_{\tau_2} \end{cases} \quad (2.5)$$

where $a_1$, $a_2$, $b_1$, $b_2$ and c are constants. and the delay times of x and y can be represented as $\tau_1$ and $\tau_2$, respectively. The chaotic behaviors are also changed when the time delays are varied.

Now, consider a fractional order modified Double Ikeda system. Here, the conventional derivatives in Eq.(2.5) are replaced by the fractional derivatives as follows:

$$\begin{cases} \dfrac{d^{q_1} x}{dt^{q_1}} = -a_1 x - b_1 \sin x_{\tau_1} - c \sin y \\ \dfrac{d^{q_2} y}{dt^{q_2}} = -a_2 y - b_2 \sin y_{\tau_2} \end{cases} \quad (2.6)$$

where $q_1, q_2$ are two fractional order numbers.

In this paper, we analyse and present simulation results of the chaotic dynamics produced from a new fractional Double Ikeda system as the fractional order derivatives $q_1, q_2$ in the state equations of Eq. (2.6) is varied from 1 to 0.1.

## 2.4 Simulation Results

We vary the derivative orders $q_1, q_2$ and the system parameter *c*. Other system parameters are fixed, which are given as: $a_1 = 1$, $a_2 = 15$, $b_1 = b_2 = 20$, $\tau_1 = \tau_2$ =2. The numerical simulations are carried out by MATLAB with using the fractional operator in table I of [73] in the Simulink environment.

The phase portraits, Poincaré maps and bifurcation diagrams of the systems with total order of derivatives from 2~0.2 are showed in Fig.2.1~Fig.2.10. Chaos exists for all cases. The period 2 phase portraits in Fig.2.1(b), Fig.2.2(b), Fig.2.3(b) seems contradictory with the “four lines” bifurcations in Fig.2.1(d), Fig.2.2(d), Fig.2.3(d), respectively. Actually, the “four lines” are dotted lines, the corresponding two dotted lines form a undotted line. Therefore period 2 motions also appear in Fig.2.1(d), Fig.2.2(d), Fig.2.3(d).

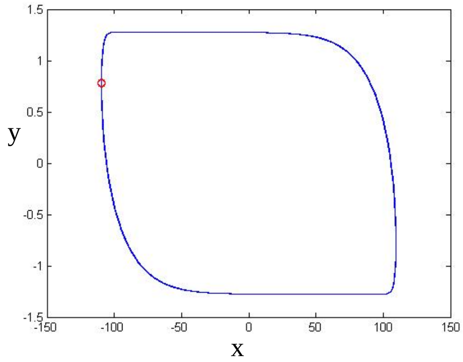


(a) *Period 1, c=151*

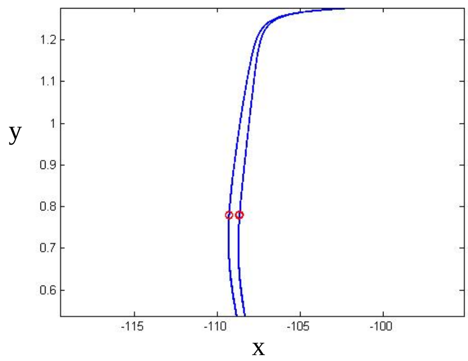


(b) *Period 2, c=152*

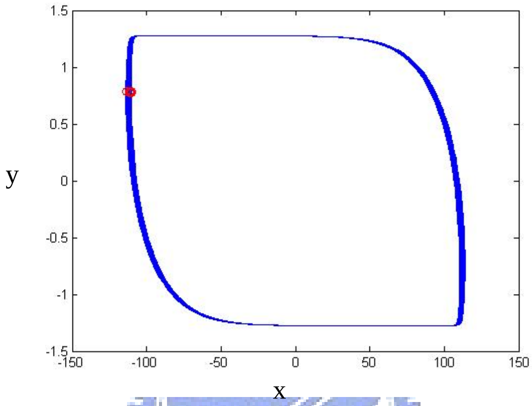


(c) *Chaos, c=157*

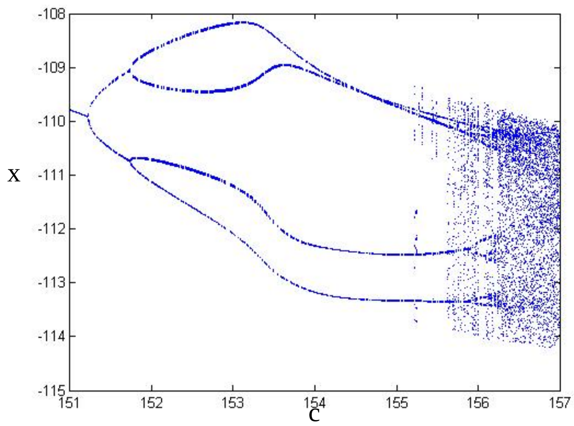


(d)

Fig. 2.1 The phase portraits and the bifurcation diagram for double Ikeda system with order $q_1 = 1$ and $q_2 = 1$. The first bifurcation point c=151.2. The second bifurcation point c=151.7. The third bifurcation point c=155.7.

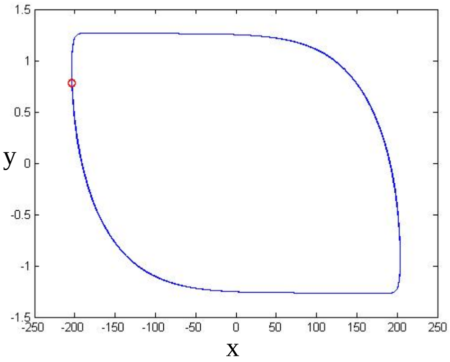


(a) *Period 1, c=292*

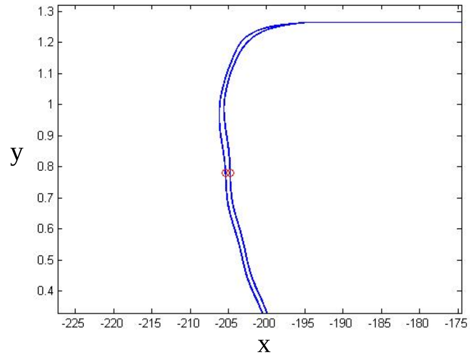


(b) *Period 2, c=294*

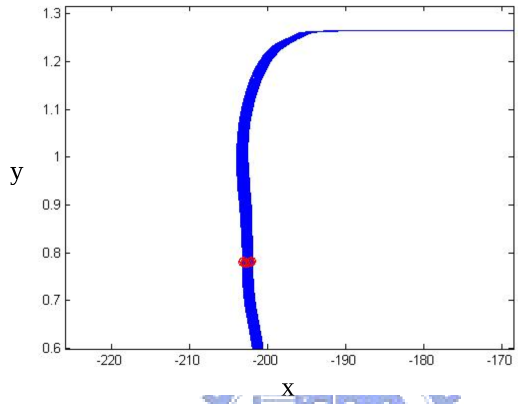


(c) *Chaos, c=291*

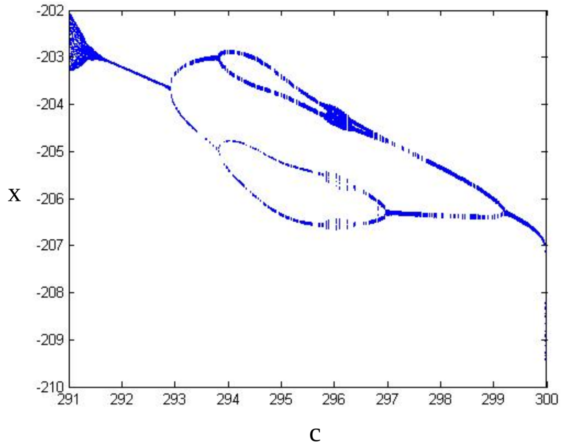


(d)

Fig. 2.2 The phase portraits and the bifurcation diagram for double Ikeda system with order $q_1 = 0.9$ and $q_2 = 0.9$. The first bifurcation point c=292.9. The second bifurcation point c=293.8. The third bifurcation point c=297.1. The fourth bifurcation point c=299.2.

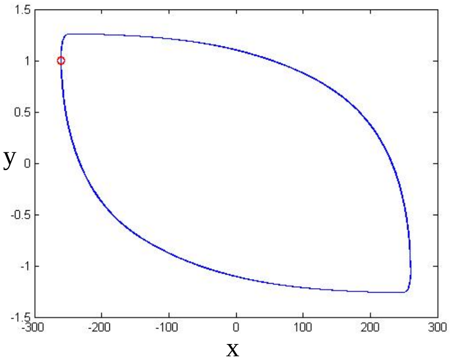


(a) *Period 1, c=412*

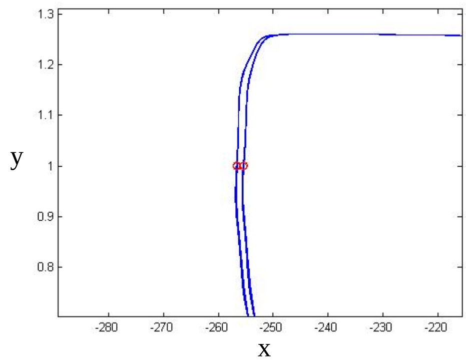


(b) *Period 2, c=410*

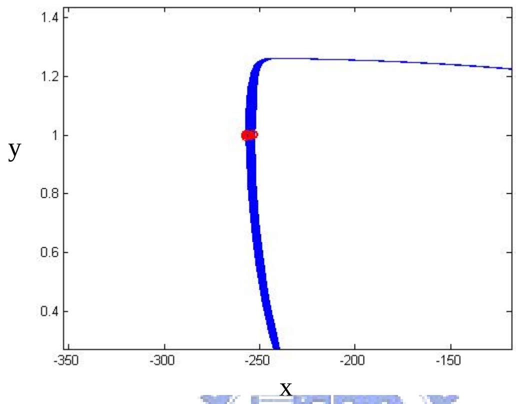


(c) *Chaos, c=405*

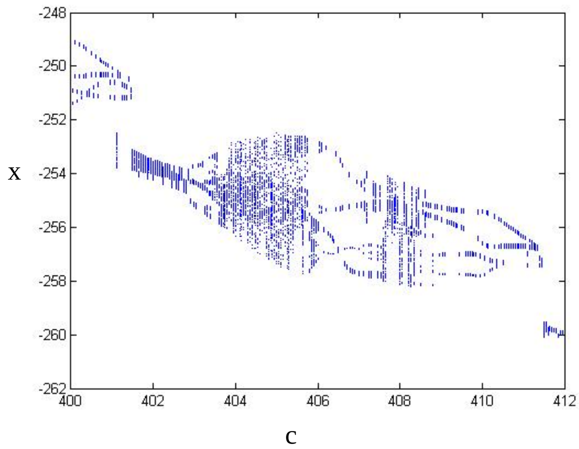


(d)

Fig. 2.3 The phase portraits and the bifurcation diagram for double Ikeda system with order $q_1 = 0.8$ and $q_2 = 0.8$. The first bifurcation point c=411.4.

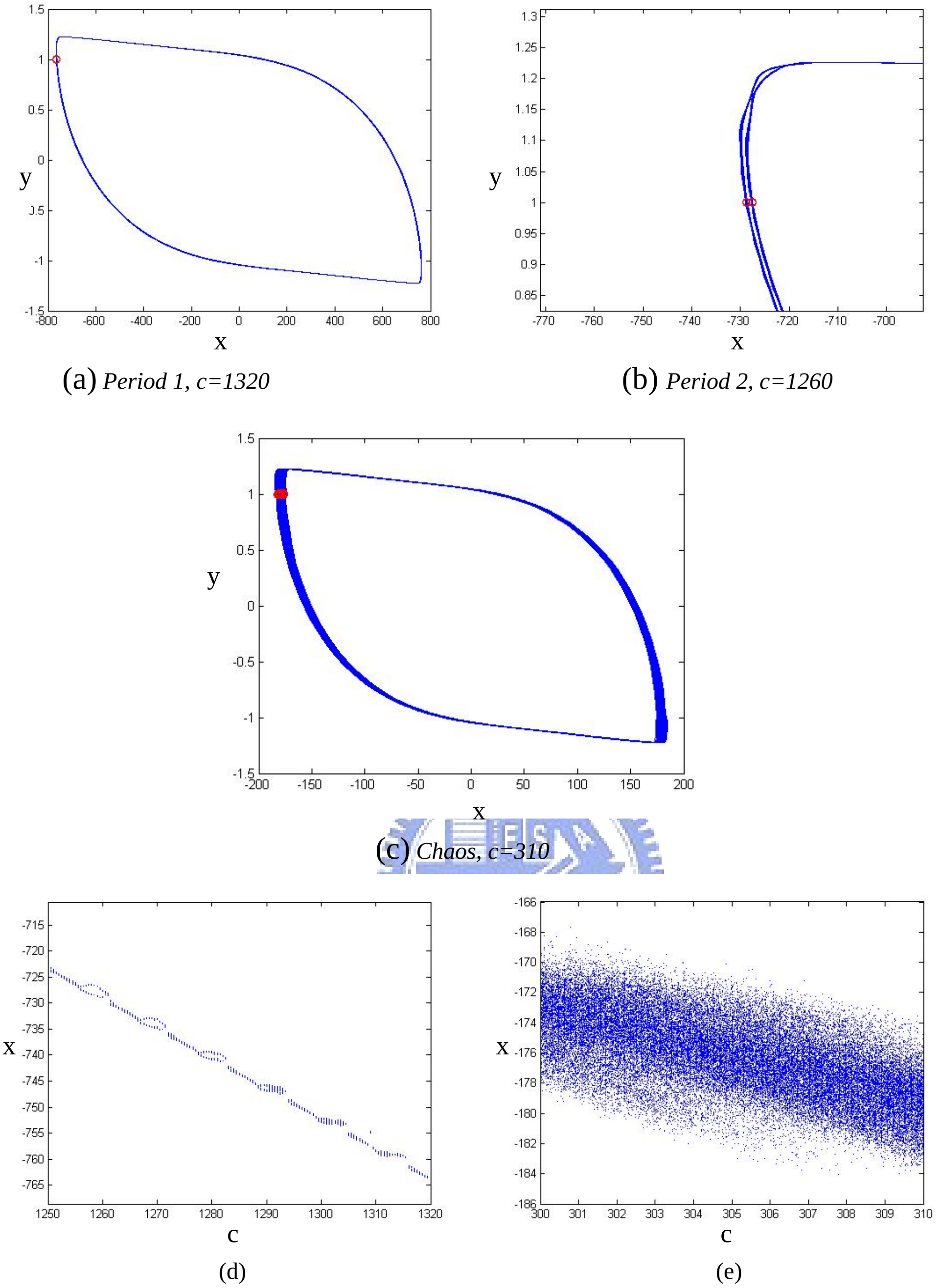


Fig. 2.4 The phase portraits and the bifurcation diagram for double Ikeda system with order $q_1 = 0.7$ and $q_2 = 0.7$ . The first bifurcation point c=1256. The second bifurcation point c=512.

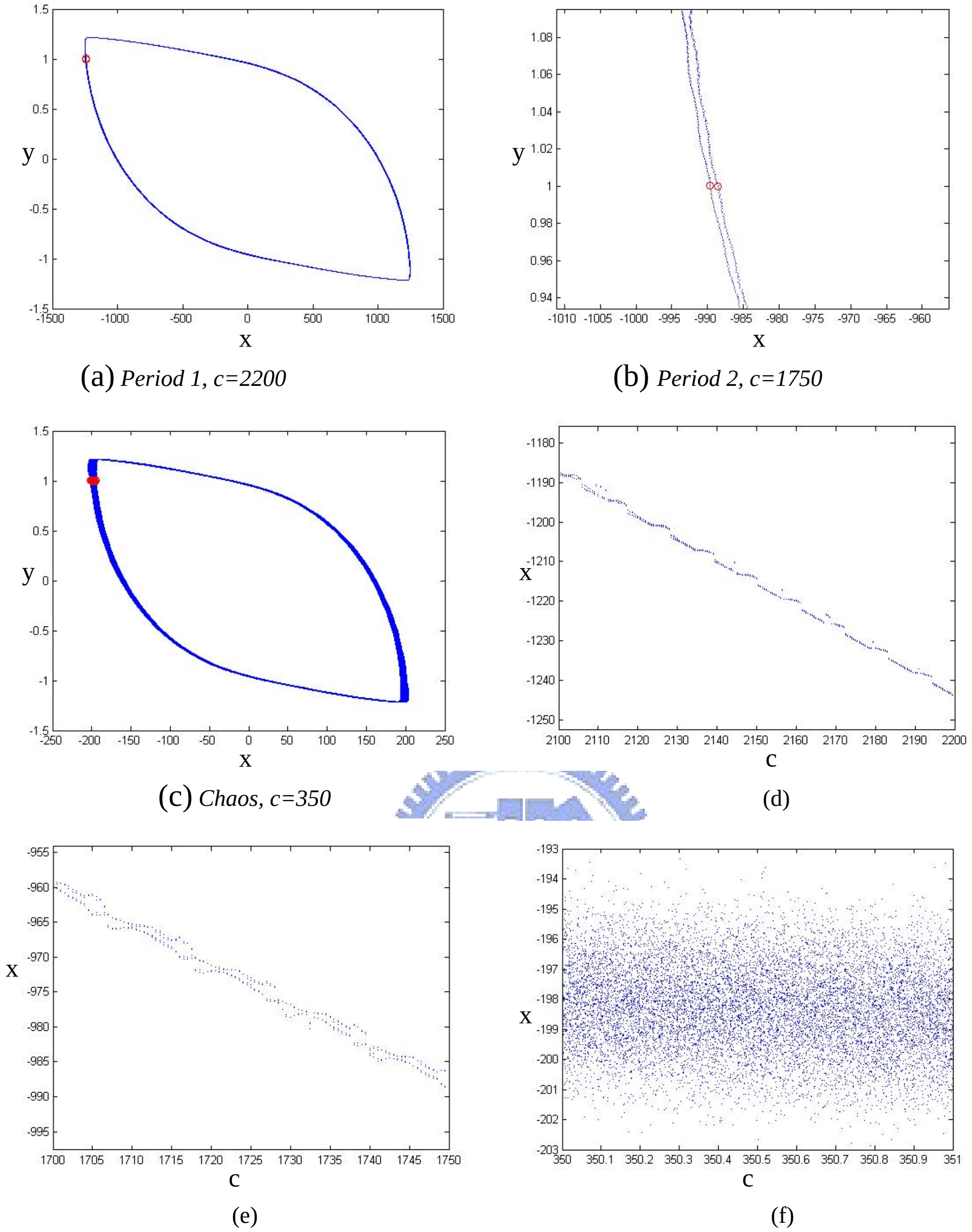


Fig. 2.5 The phase portraits and the bifurcation diagram for double Ikeda system with order $q_1 = 0.6$ and $q_2 = 0.6$. The first bifurcation point c=1821. The second bifurcation point c=437.

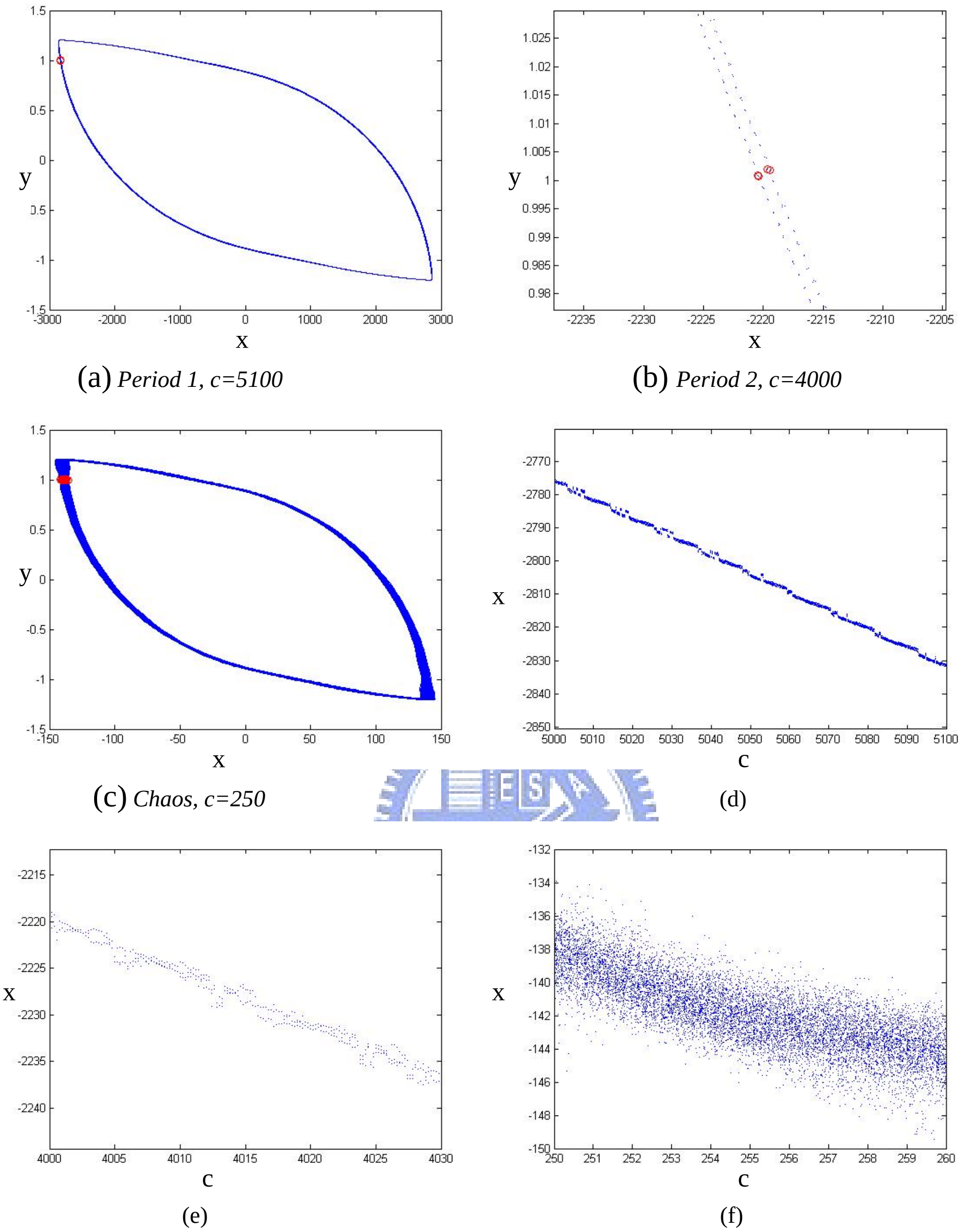

(a) *Period 1, c=5100* (b) *Period 2, c=4000*

(c) *Chaos, c=250* (d)

(e) (f)

Fig. 2.6 The phase portraits and the bifurcation diagram for double Ikeda system with order $q_1 = 0.5$ and $q_2 = 0.5$ . The first bifurcation point c=4316. The second bifurcation point c=334.

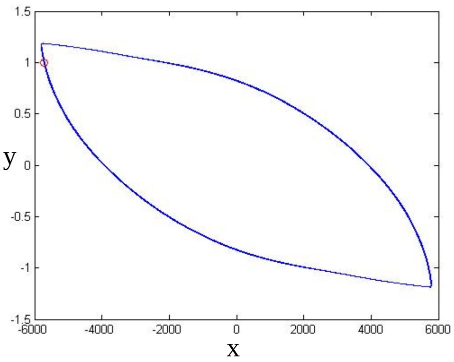


(a) *Period 1, c=11000*

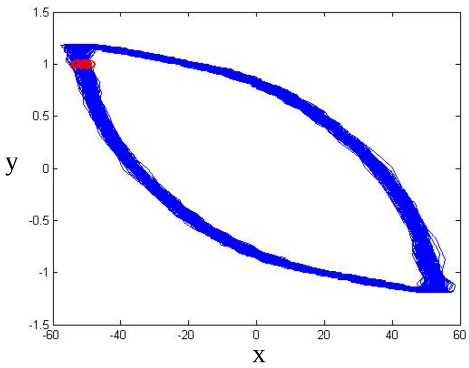


(b) *Chaos, c=100*

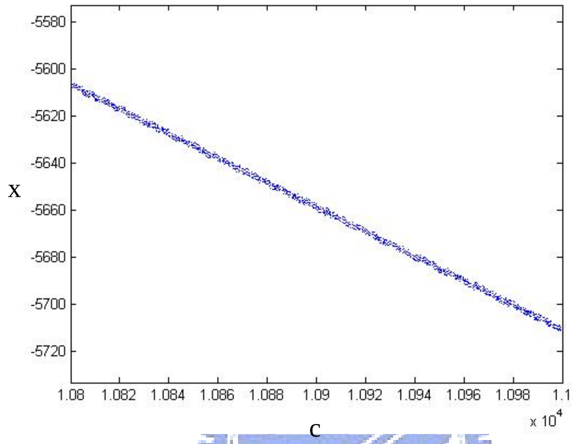


(c)

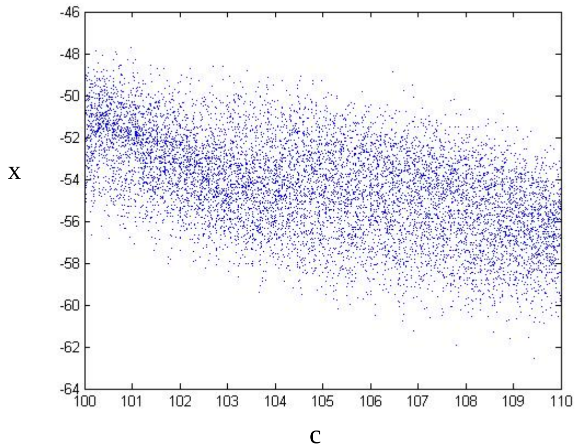


(d)

Fig. 2.7 The phase portraits and the bifurcation diagram for double Ikeda system with order $q_1 = 0.4$ and $q_2 = 0.4$. The first bifurcation point c=211.

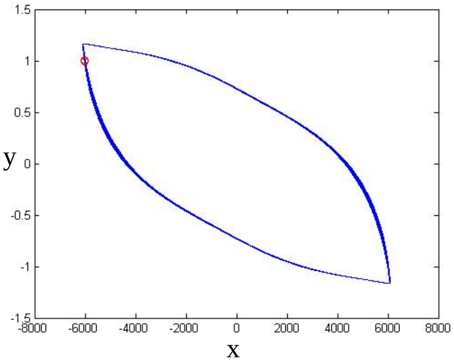


(a) *Period 1, c=12030*

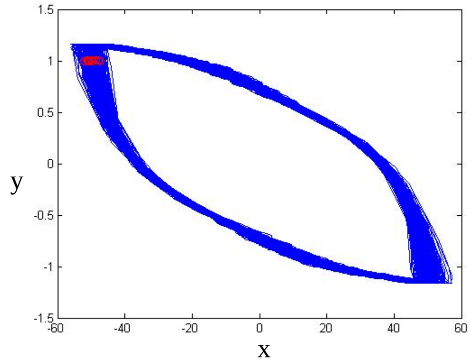


(b) *Chaos, c=100*

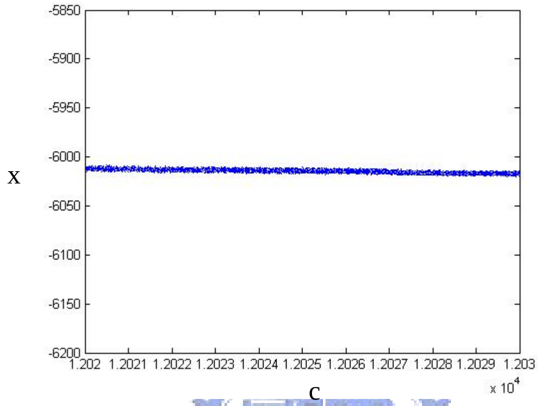


(c)

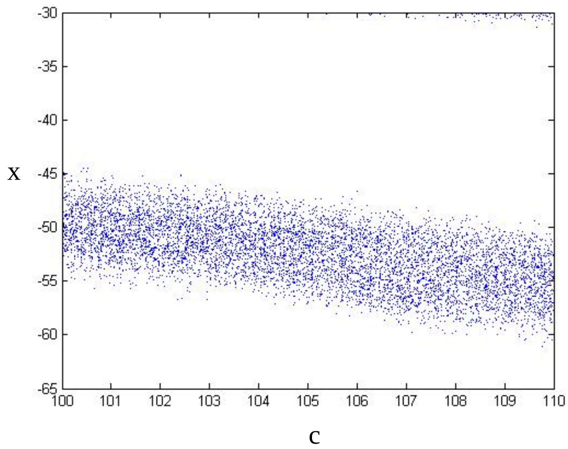


(d)

Fig. 2.8 The phase portraits and the bifurcation diagram for double Ikeda system with order $q_1 = 0.3$ and $q_2 = 0.3$. The first bifurcation point c=225.

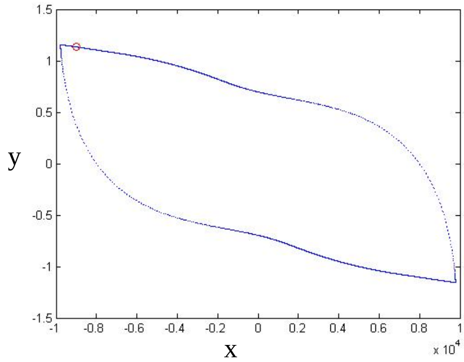


(a) *Period 1, c=20010*

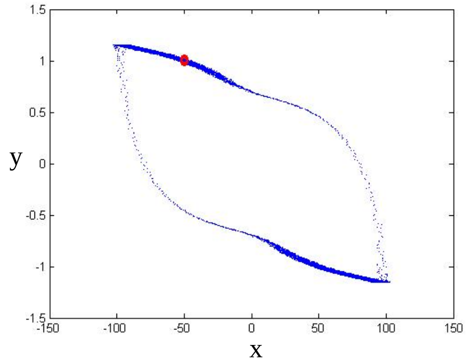


(b) *Chaos, c=200*

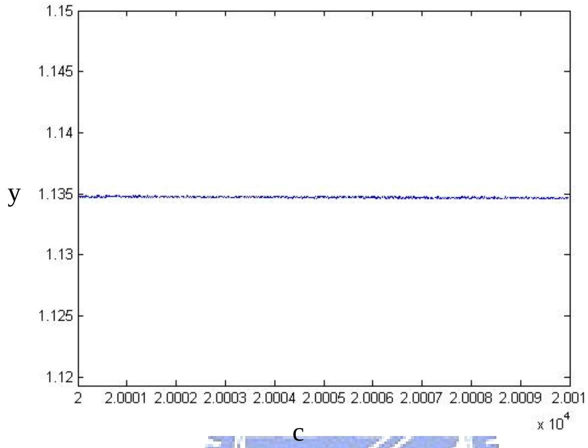


(c)

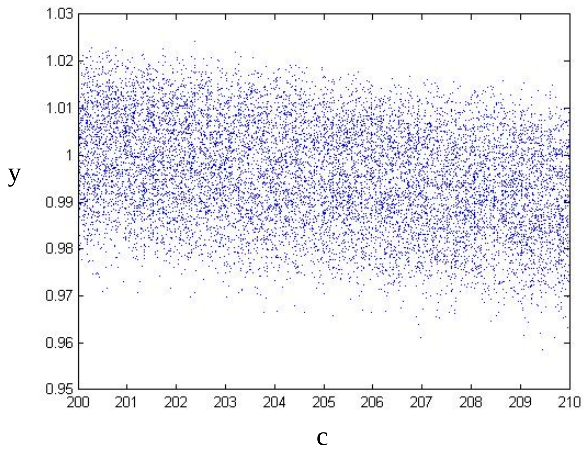


(d)

Fig. 2.9 The phase portraits and the bifurcation diagram for double Ikeda system with order $q_1 = 0.2$ and $q_2 = 0.2$. The first bifurcation point c=230.

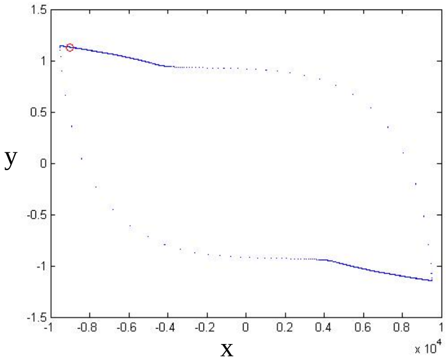


(a) *Period 1, c=20010*

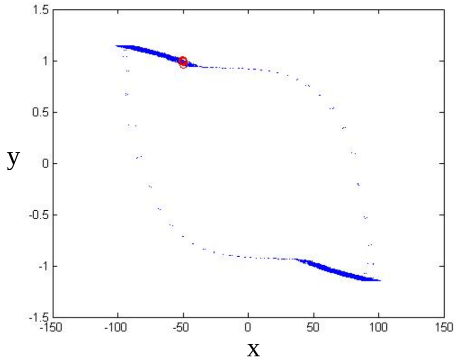


(b) *Chaos, c=200*

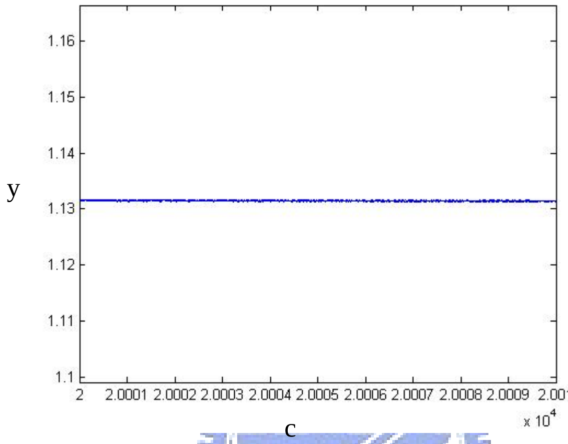


(c)

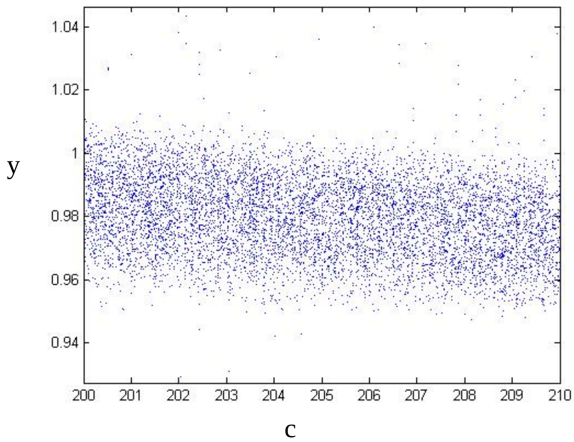


(d)

Fig. 2.10 The phase portraits and the bifurcation diagram for double Ikeda system with order $q_1 = 0.1$ and $q_2 = 0.1$. The first bifurcation point c=232.

# Chapter 3

# Lag and Anticipated Synchronization and Anti-synchronization of Two Uncoupled Time-delayed Chaotic Systems

## 3.1 Preliminaries

Lag and anticipated synchronization and lag and anticipated anti-synchronization are newly discovered in two identical double Ikeda systems with different initial conditions without any control scheme and coupling terms. There are two situations for all possible initial conditions. They are the lag or anticipated synchronization, the lag or anticipated anti-synchronization.

## 3.2 Lag or anticipated synchronization and lag or anticipated anti-synchronization

Consider the first time-delay chaotic system

$$\dot{x} = f(x, x_\tau, t) \tag{3.1}$$

and second time-delay chaotic system

$$\dot{y} = f(y, y_\tau, t) \tag{3.2}$$

where $x, y \in R^n$ are $n$-dimensional state vectors, $x_\tau = x(t-\tau)$ are corresponding time-delay state vectors. The error are defined as $e = x(t-T) - y(t)$. If the following conditions hold, the systems are in lag synchronization.

$$e_i = x_{iT_i} - y_i = 0\,, \quad i = 1,2,...., p \le n \tag{3.3}$$

where $x_i$, $y_i$ are the state vectors of the system, $T_i$ is the time which $x_i$ lag behind $y_i$. When $T_i$ is negative, we have anticipated synchronization.

In the case of anti-synchronization, the states of the systems which have opposite signs, the error $e = x(t-T) + y(t)$ will converge to zero. Therefore, we can say the lag anti-synchronization is achieved when the following conditions are satisfied:

$$e_i = x_{iT_i} + y_i = 0, \quad i = 1,2,...., p \le n \tag{3.4}$$

where $x_i$, $y_i$ are the state vectors of the system, $T_i$ is the time which $x_i$ lag behind $y_i$. When $T_i$ is negative, we have anticipated anti-synchronization.

## 3.3 The lag or anticipated synchronization of two identical double Ikeda systems

We consider two double Ikeda systems which consist of two coupled Ikeda equations:

System A

$$\begin{cases} \dot{x}_1 = -a_1 x_1 - b_1 \sin x_{1_{\tau_1}} - c \sin y_1 \\ \dot{y}_1 = -a_2 y_1 - b_2 \sin y_{1_{\tau_2}} \end{cases} \tag{3.5}$$

and system B

$$\begin{cases} \dot{x}_2 = -a_1 x_2 - b_1 \sin x_{2_{\tau_1}} - c \sin y_2 \\ \dot{y}_2 = -a_2 y_2 - b_2 \sin y_{2_{\tau_2}} \end{cases} \tag{3.6}$$

with positive $a_{1,2}$ and $b_{1,2}$

This investigation is of considerable practical importance, as the equations of the class B lasers with feedback (typical representatives of class B are solid-state, semiconductor, and low pressure CO2 lasers [74]) can be reduced to an equation of the Ikeda type [75].

The Ikeda model was introduced to describe the dynamics of an optical bistable resonator, plays an important role in electronics and physiological studies and is well-known for delay-induced chaotic behavior [76,77,78,79]. Physically x is the phase lag of the electric field across the resonator; $a$ is the relaxation coefficient for the driving x and driven y dynamical variables; $b_{1,2}$ are the laser intensities injected into the driving and driven systems, respectively. $\tau_{1,2}$ are the feedback delay times in the coupled systems.

We keep the delay time fixed in 2 second ($\tau = 2$) and the parameters are shown as follows: $a_1 = 1$，$a_2 = 15$，$b_1 = 20$，$b_2 = 20$，$c = 157$. The system is chaotic in foregoing conditions as shown in Fig. 3.1. The numerical simulations are carried out by MATLAB, The initial conditions we choose are constant.

Fig.3.2 shows the time histories of double Ikeda system with initial conditions as follows in Table 1. Fig.3.2 (b) is the magnified diagram of Fig.3.2 (a). After 180 sec, state variables of system A become in lag synchronization with that of the system B. Lag of $x_1$ to $x_2$ is 0.14868 sec. And lag of $y_1$ to $y_2$ is 0.14868 sec. The situation remain unchanged until 20000 sec. From Fig. 3.2, we can see the lag synchronization in Case 1~8 by Table 3.1. From Fig.3.2 (b), state variables of system A is in lag synchronization with that of system B, or state variables of system B is in anticipated synchronization with that of system A.

Table 3.1 The initial condition of lag or anticipated synchronization.

| Case | $x_1$ | $y_1$ | $x_2$ | $y_2$ |
|---|---|---|---|---|
| 1 | 1 | 1 | 0.000000001 | 0.000000001 |
| 2 | 1 | 1 | -0.000000001 | 0.000000001 |

| | | | | |
|---|---|---|---|---|
| 3 | 1 | -1 | 0.000000001 | -0.000000001 |
| 4 | 1 | -1 | -0.000000001 | -0.000000001 |
| 5 | -1 | 1 | 0.000000001 | 0.000000001 |
| 6 | -1 | 1 | -0.000000001 | 0.000000001 |
| 7 | -1 | -1 | 0.000000001 | -0.000000001 |
| 8 | -1 | -1 | -0.000000001 | -0.000000001 |

### 3.4 The lag or anticipated anti-synchronization of two identical double Ikeda systems

In this section, we change the initial conditions. The lag anti-synchronization is occurred. Fig.3.3 shows the time histories of double Ikeda system with initial conditions as follows in Table 3.2. Fig.3.3 (b) is the magnified diagram of Fig.3.3 (a). Fig.3.3 (c) is the time history of $-x_1$ (blue) and $x_2$ (red), $-y_1$ (blue) and $y_2$ (red) of double Ikeda systems. Lag of $x_1$ to $x_2$ is 0.14868 sec. And lag of $y_1$ to $y_2$ is 0.14868 sec. The situation remain unchanged until 20000 sec. From Fig. 3.3, we can see the lag synchronization in Case 9~16 by Table 2. From Fig.3.3 (b), state variables of system A is in lag anti-synchronization with that of system B, or state variables of system B is in anticipated anti-synchronization with that of system A.

Table 3.2 The initial condition of lag or anticipated anti-synchronization.

| Case | $x_1$ | $y_1$ | $x_2$ | $y_2$ |
|---|---|---|---|---|
| 9 | 1 | 1 | 0.000000001 | -0.000000001 |
| 10 | 1 | 1 | -0.000000001 | -0.000000001 |
| 11 | 1 | -1 | 0.000000001 | 0.000000001 |
| 12 | 1 | -1 | -0.000000001 | 0.000000001 |

| | | | | |
|---|---|---|---|---|
| 13 | -1 | 1 | 0.000000001 | -0.000000001 |
| 14 | -1 | 1 | -0.000000001 | -0.000000001 |
| 15 | -1 | -1 | 0.000000001 | 0.000000001 |
| 16 | -1 | -1 | -0.000000001 | 0.000000001 |

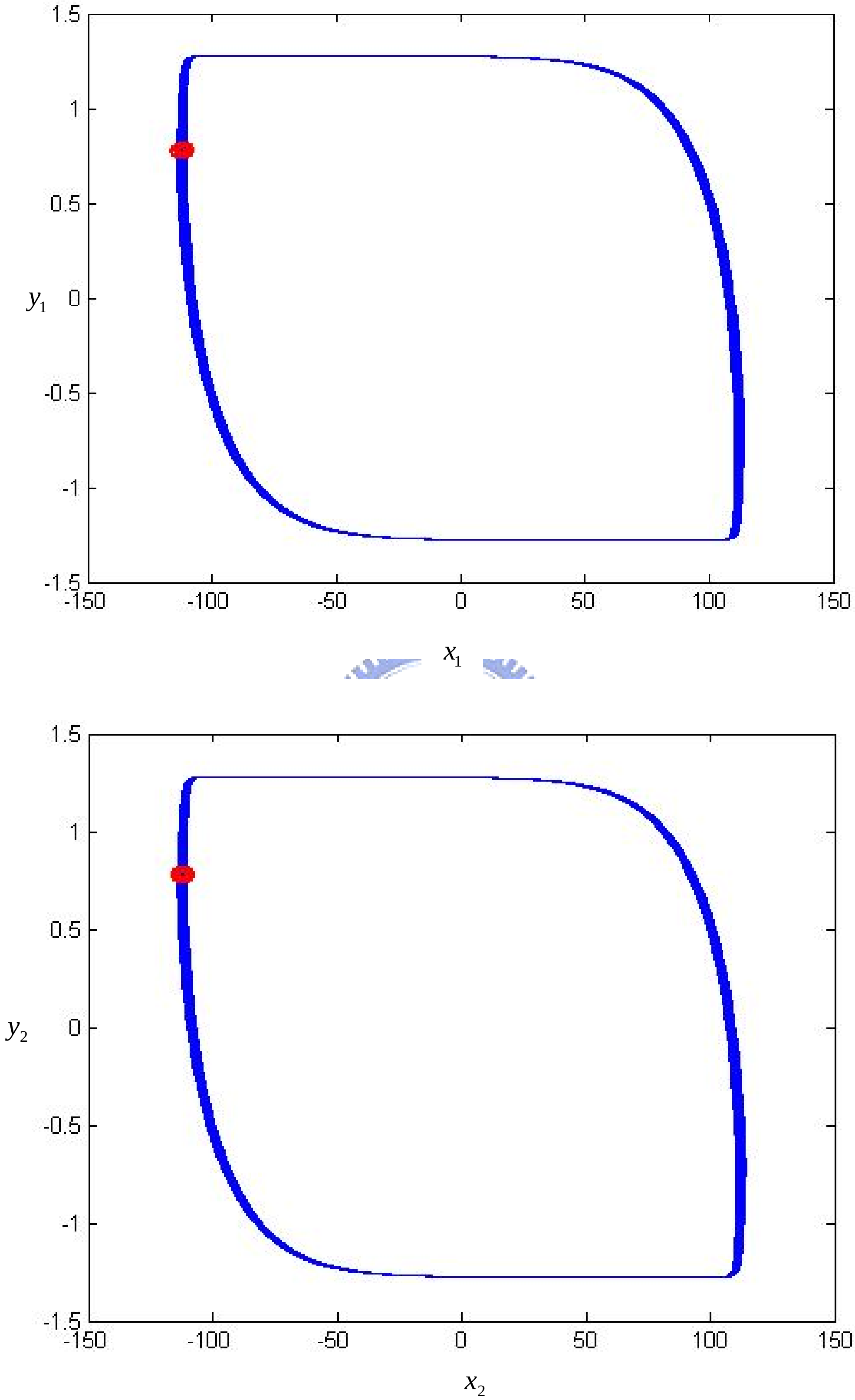


Fig. 3.1 The phase portraits diagram for double Ikeda system.

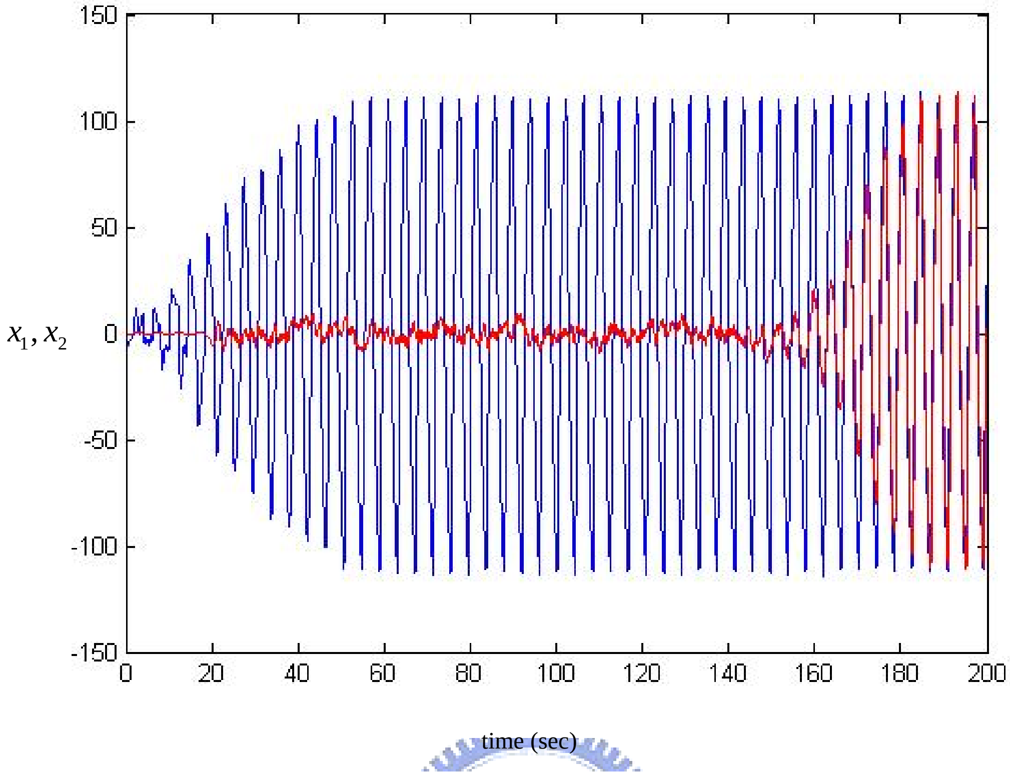


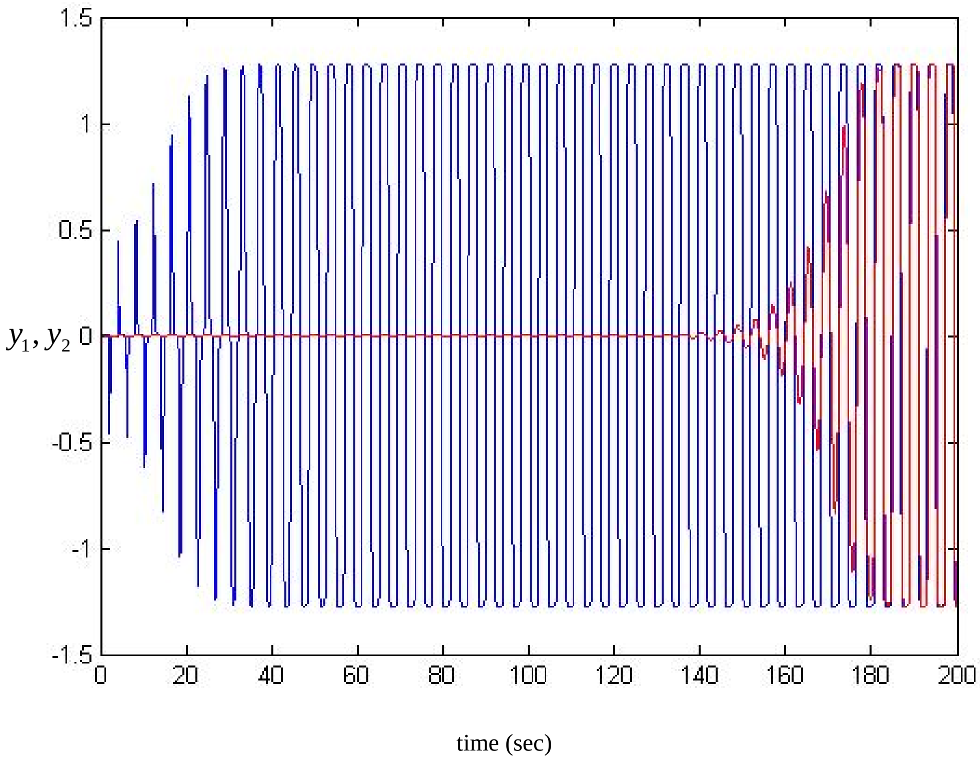


Fig.3.2 (a) The time histories of $x_1$ (blue) and $x_2$ (red), $y_1$ (blue) and $y_2$ (red) of double Ikeda systems with initial conditions in Table 3.1.

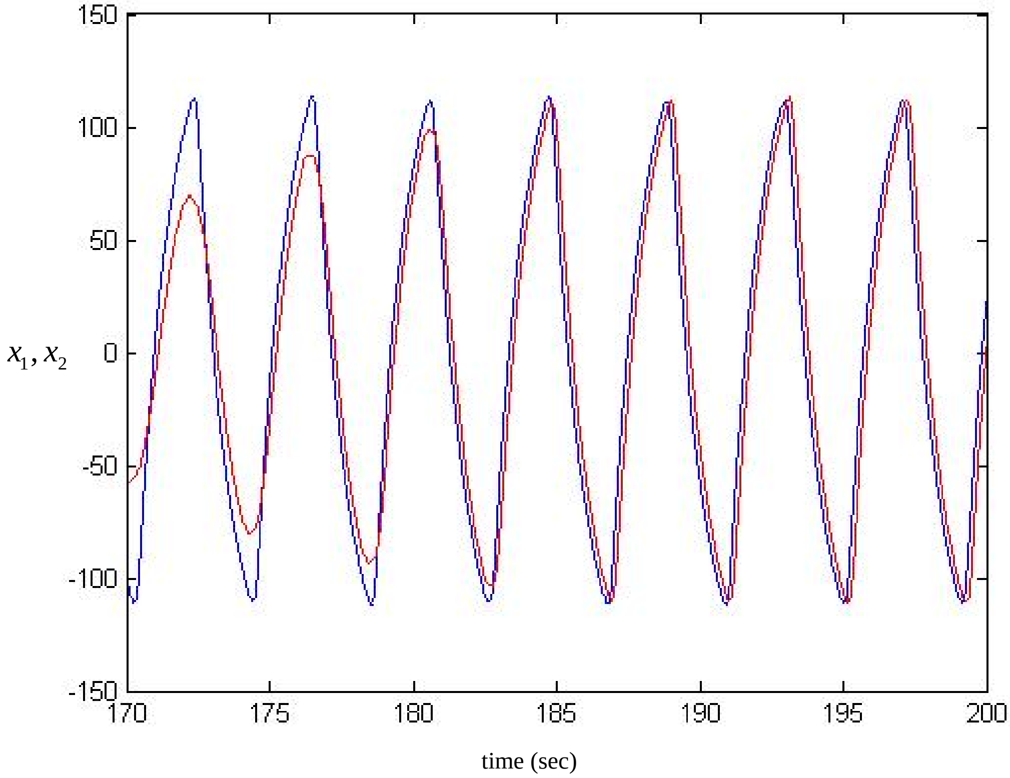


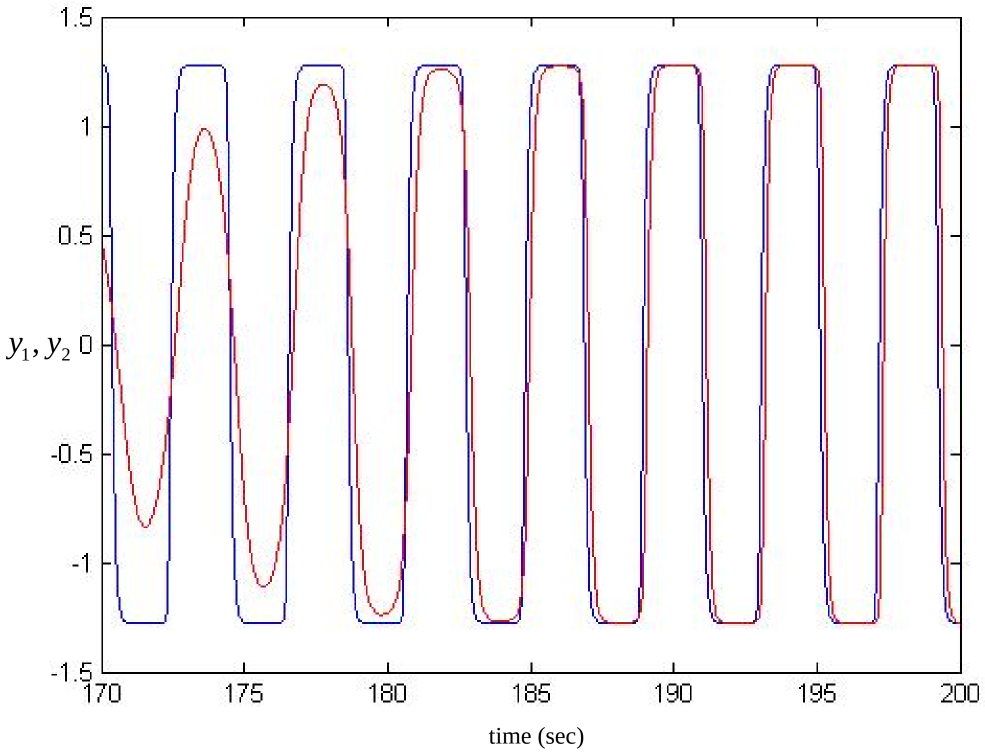


Fig.3.2 (b) The time histories of $x_1$ (blue) and $x_2$ (red), $y_1$ (blue) and $y_2$ (red) of double Ikeda systems with initial conditions in Table 3.1.

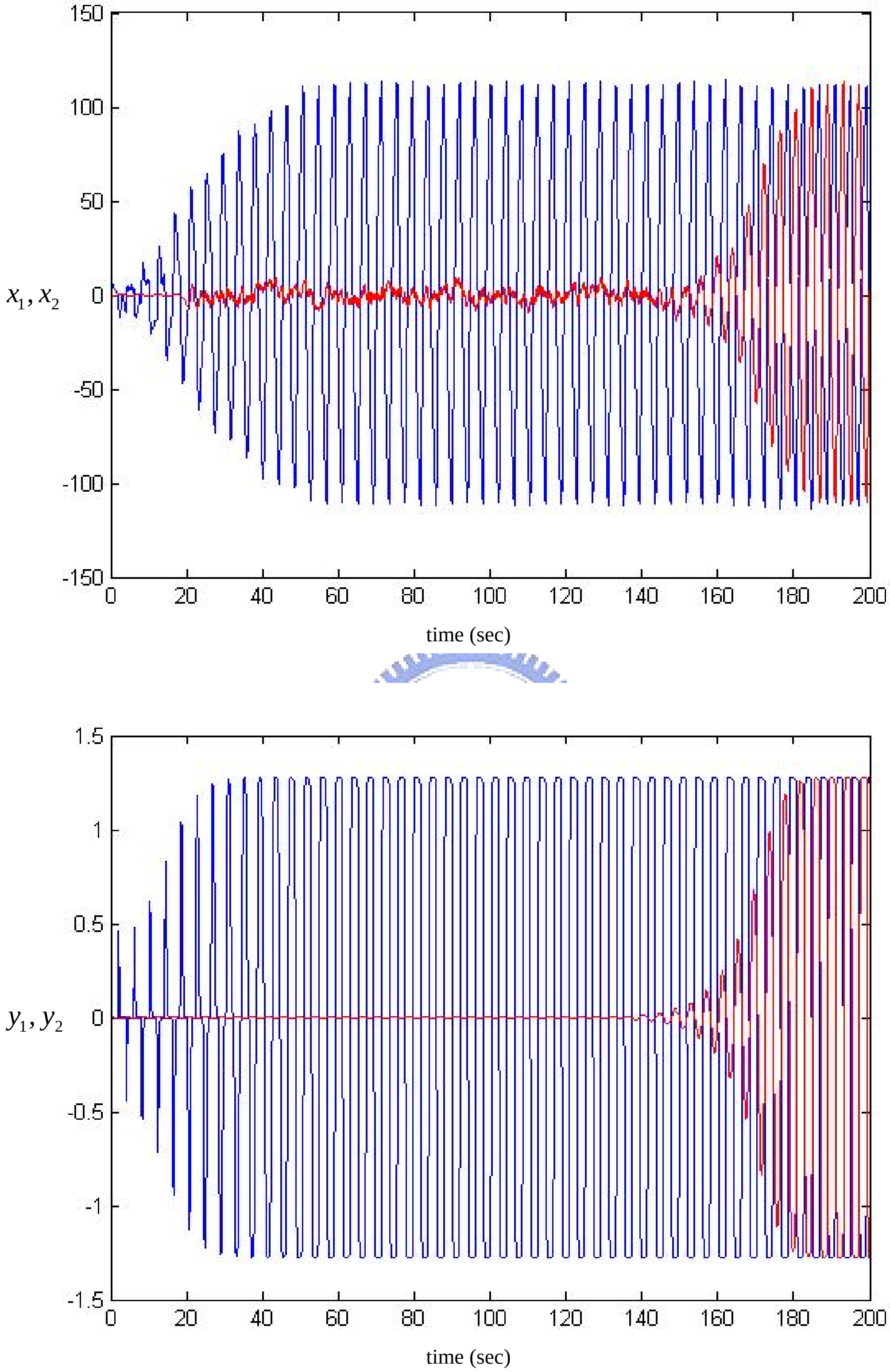


Fig.3.3 (a) The time histories of $x_1$ (blue) and $x_2$ (red), $y_1$ (blue) and $y_2$ (red) of double Ikeda systems with initial conditions in Table 3.2.

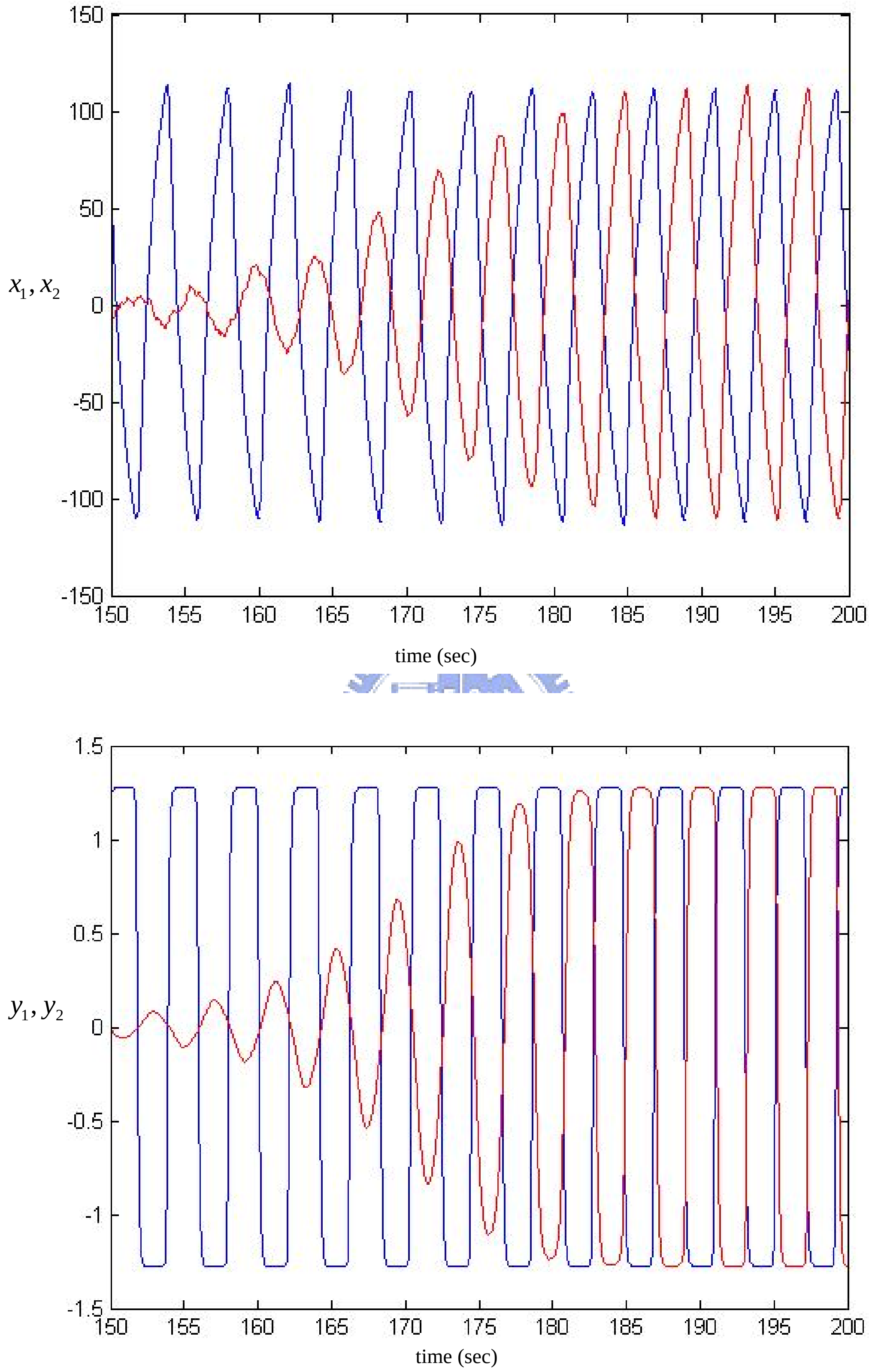


Fig.3.3 (b) The time histories of $x_1$ (blue) and $x_2$ (red), $y_1$ (blue) and $y_2$ (red) of double Ikeda systems with initial conditions in Table 3.2.

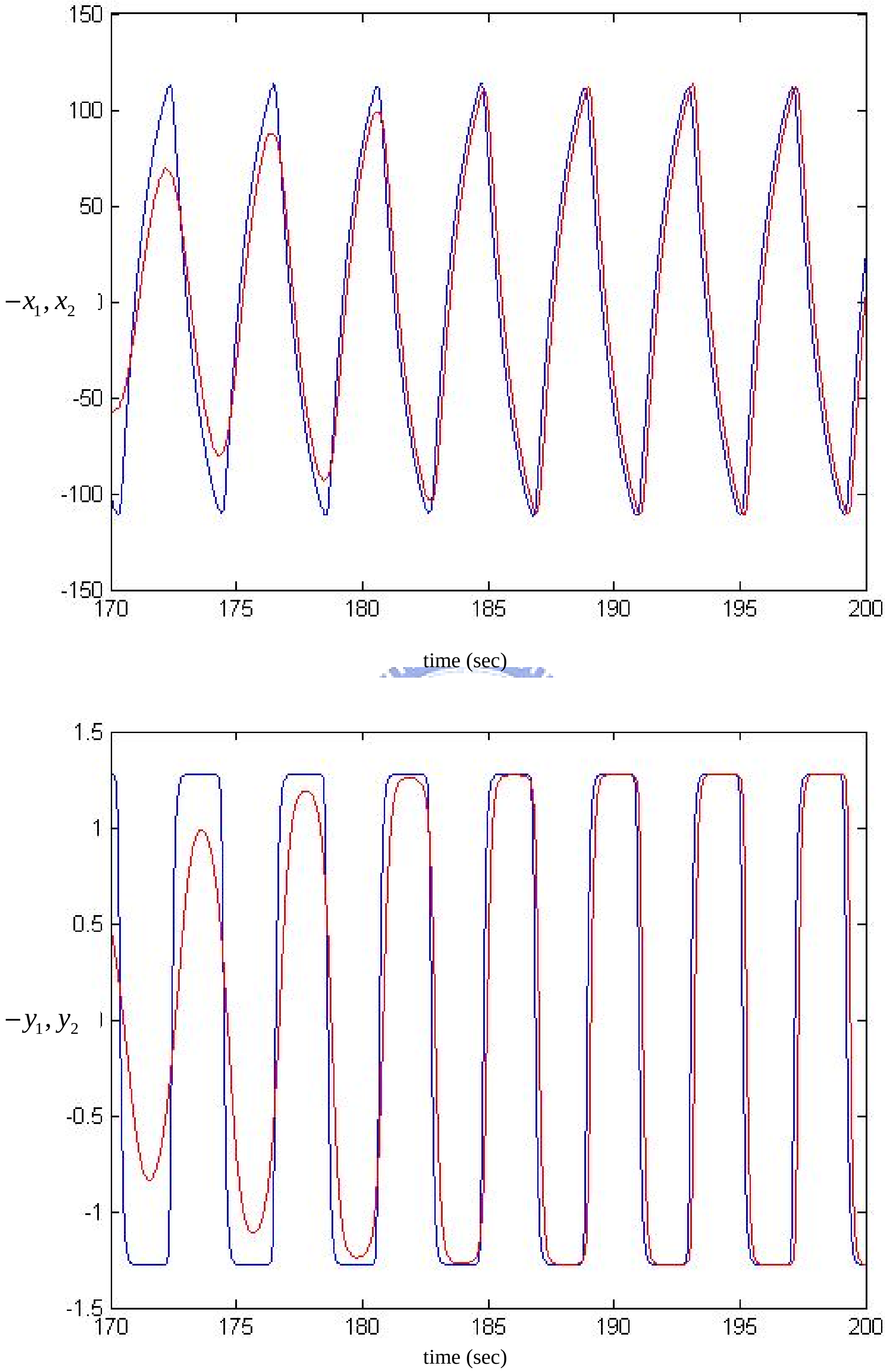


Fig.3.3 (c) The time histories of $-x_1$ (blue) and $x_2$ (red), $-y_1$ (blue) and $y_2$ (red) of double Ikeda systems with initial conditions in Table 3.2.

# Chapter 4

# Chaos and Chaotization of a Double Ikeda System by Chaotic Delay Time

## 4.1 Preliminaries

In this Chapter, the chaotization of a double Ikeda delay system by replacing the original constant delay time by a function of chaotic state variable of a second double Ikeda chaotic system. It is found that chaos exists for many cases.

## 4.2 Chaos of a double Ikeda system

According to Chapter 3, we consider two double Ikeda systems which consist of two coupled Ikeda equations:

$$\begin{cases} \dot{x}_1 = -a_1 x_1 - b_1 \sin x_{1_{\tau_1}} - c \sin y_1 \\ \dot{y}_1 = -a_2 y_1 - b_2 \sin y_{1_{\tau_2}} \end{cases} \tag{4.1}$$

and

$$\begin{cases} \dot{x}_2 = -a_1 x_2 - b_1 \sin x_{2_{\tau_1}} - d \sin y_2 \\ \dot{y}_2 = -a_2 y_2 - b_2 \sin y_{2_{\tau_2}} \end{cases} \tag{4.2}$$

The scheme is to replace the constant delay time $\tau_1$ or $\tau_2$ in system (4.1) by a function of a chaotic state of system (4.2).

## 4.3 Chaotization scheme of a double Ikeda system by chaotic delay time

Creating chaos is called chaotization at times. The above replacements enhance the existing chaos of the originally system effectively. The results are demonstrated by numerical results.

In order to induce chaotic phenomena of the double Ikeda system (4.1), $p+qx_2$ and $p+qy_2$ replace the delay times in system (4.1) respectively, where *p*, *q* are constant.

## 4.4 Numerical Simulations for Chaos and Chaotization by time delay driven by a chaotic signal

In following simulations, we replace the delay time in system (4.1) by $x_2$ where $x_2$ is a state variable in system (4.2). In our numerical simulations, $a_1=1$, $a_2=15$, $b_1=20$, $b_2=20$, $c=157$, $\tau_1=\tau_2=2s$ of system (4.1) and (4.2) are fixed. The initial states of system (4.1) and (4.2) are $x_1(0)=-1$, $y_1(0)=-1$, $x_2(0)=-1.1$, $y_2(0)=-1.1$. The numerical simulations are carried out by MATLAB.

Case 1 : The parameters $a_1=1$, $a_2=15$, $b_1=20$, $b_2=20$, $c=157$, $d=157$ of system (4.1) and (4.2) are fixed. The delay time $\tau_1$ of system (4.1) is replaced by $200+x_2$, where $x_2$ is the state variable of system (4.2). The phase portraits are shown in Fig. 4.1. The phase portrait with the original constant delay time is shown in Fig. 4.1(b)

Case 2 : The parameters $a_1=1$, $a_2=15$, $b_1=20$, $b_2=20$, $c=157$, $d=157$ of system (4.1) and (4.2) are fixed. The delay time $\tau_2$ of system (4.1) is replaced by $200+x_2$, where $x_2$ is the state variable of system (4.2). The phase portraits are shown in Fig. 4.2.

Case 3~4 : The delay times are changed by $200+0.5x_2$, the sequences which are similar to Case 1~2. The phase portraits are shown in Fig. 4.3~4.4.

Case 5~6 : The delay times are changed by $200 + 0.612x_2$, the sequences which are similar to Case 1~2. The phase portraits are shown in Fig. 4.5~4.6.

In Case 2 and 4, it is not found that chaos exists. The time history are not conform the chaos. The time histories are shown in Fig. 4.7~4.8.

For the chaotization, we replace the delay time in system (4.1) by a function of chaotic states of system (4.2). The system (4.1) is periodic and the system (4.2) is chaotic.

Case 7 : The parameters $a_1 = 1$， $a_2 = 15$ ，$b_1 = 20$，$b_2 = 20$，$c = 151$ of system (4.1) is fixed. And the parameters $d = 157$ of system (4.2), the others are the same .The delay time $\tau_1$ of system (4.1) is replaced by $200 + 0.612x_2$, where $x_2$ is the state variable of system (4.2). The phase portraits are shown in Fig. 4.9. The phase portrait that the state is periodic is shown in Fig. 4.9(b)

Case 8 : The parameters $a_1 = 1$， $a_2 = 15$ ，$b_1 = 20$，$b_2 = 20$，$c = 151$ of system (4.1) is fixed. And the parameters $d = 157$ of system (4.2), the others are the same .The delay time $\tau_2$ of system (4.1) is replaced by $200 + 0.612x_2$, where $x_2$ is the state variable of system (4.2). The phase portraits are shown in Fig. 4.10.

Case 9~10 : The delay times are changed by $200 + 0.1y_2$, the sequences which are similar to Case 7~8. The phase portraits are shown in Fig. 4.11~4.12.

In Case 10, no chaotization exists. The time histories are shown in Fig. 4.13.

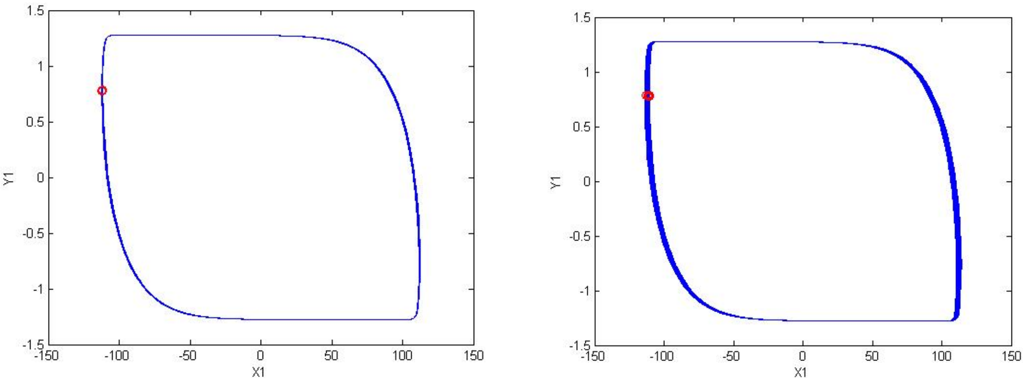


(a) (b)

Fig. 4.1 (a) The phase portrait, the delay time $\tau_1$ of system (4.1) is replaced by $200 + x_2$.

Fig. 4.1 (b) The phase portrait, the original constant delay time is fixed.

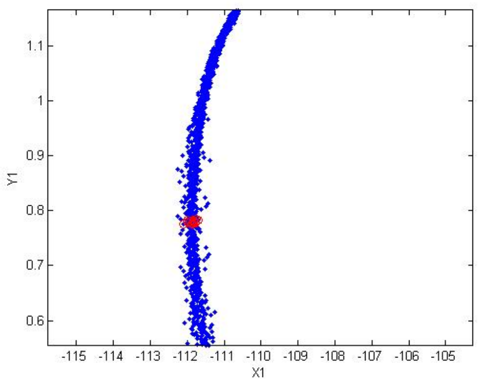


Fig. 4.1 (c) It is the magnified diagram of Fig.4.1 (a).

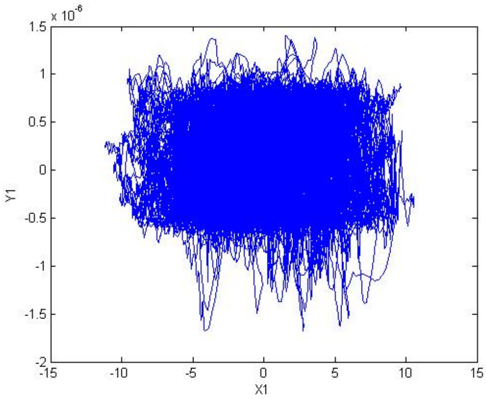


Fig. 4.2 The phase portrait, the delay time $\tau_2$ of system (4.1) is replaced by $200 + x_2$.

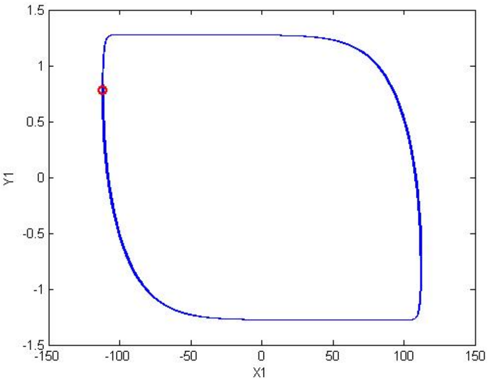


Fig. 4.3 (a) The phase portrait, the delay time $\tau_1$ of system (4.1) is replaced by $200 + 0.5x_2$.

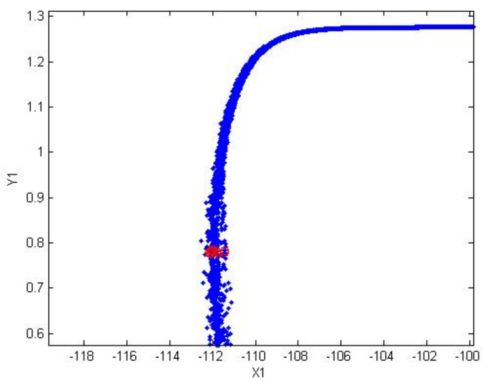


Fig. 4.3 (b) It is the magnified diagram of Fig.4.3 (a).

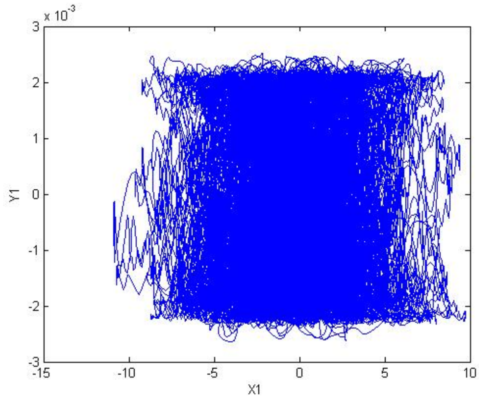


Fig. 4.4 The phase portrait, the delay time $\tau_2$ of system (4.1) is replaced by $200 + 0.5x_2$.

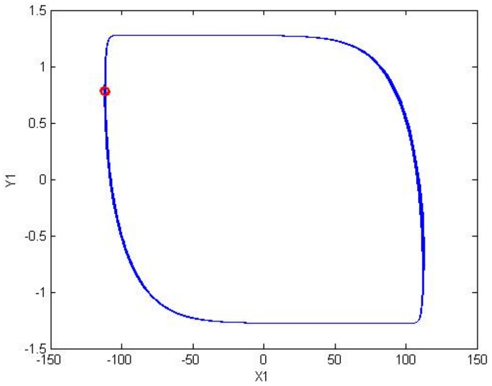


Fig. 4.5 (a) The phase portrait, the delay time $\tau_1$ of system (4.1) is replaced by $200+0.612x_2$.

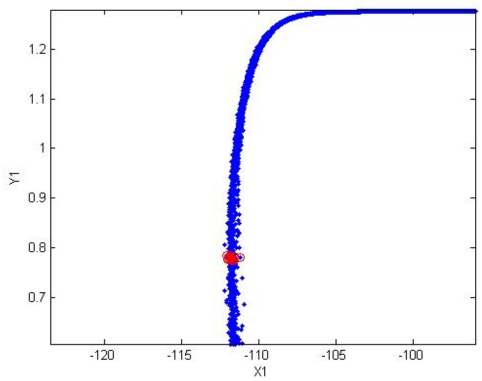


Fig. 4.5 (b) It is the magnified diagram of Fig.5 (a).

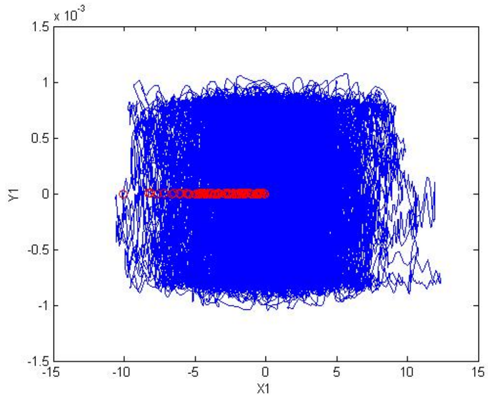


Fig. 4.6 The phase portrait, the delay time $\tau_2$ of system (4.1) is replaced by $200+0.612x_2$.

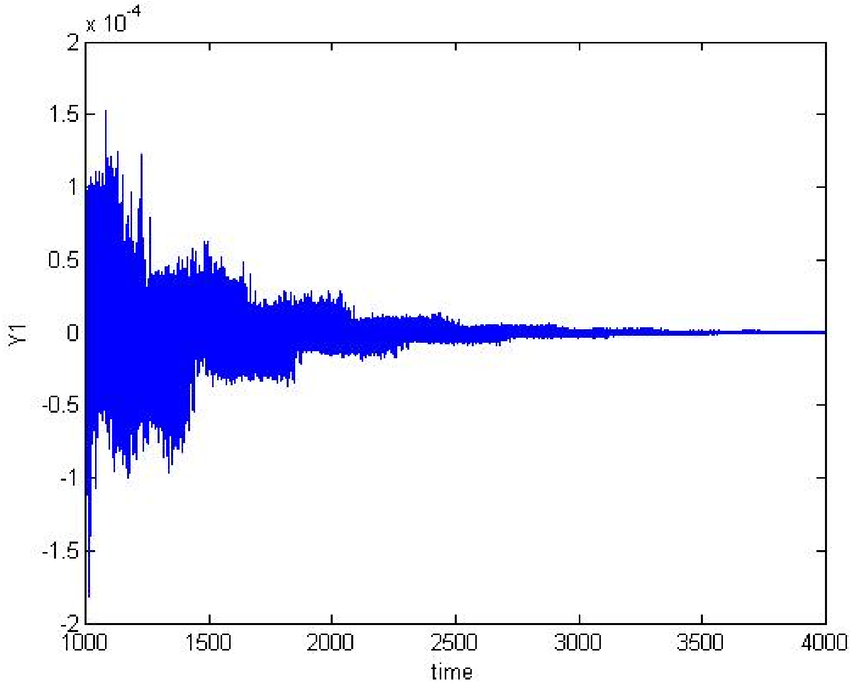


Fig. 4.7 The time history when the delay time $\tau_2$ of system (4.1) is replaced by $200 + x_2$.

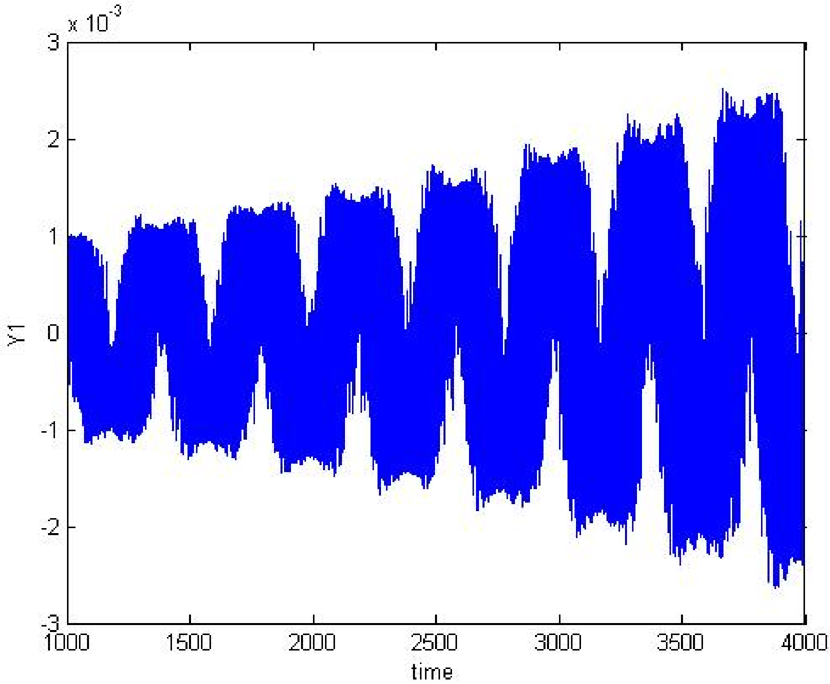


Fig. 4.8 The time history when the delay time $\tau_2$ of system (4.1) is replaced by $200 + 0.5x_2$.

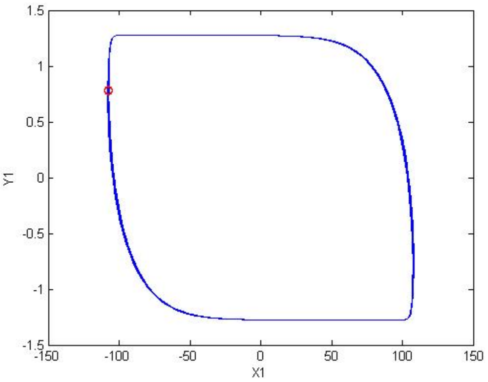


(a)

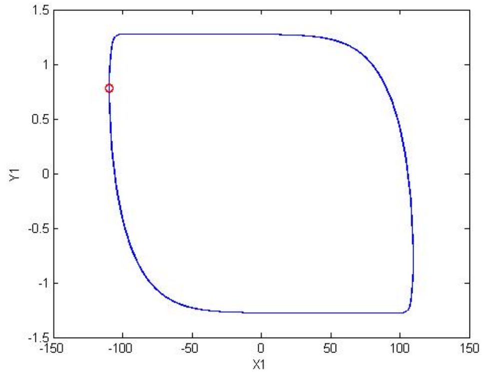


(b)

Fig. 4.9 (a) The phase portrait, the delay time $\tau_1$ of system (4.1) is replaced by $200+0.612x_2$.

Fig. 4.9 (b) The phase portrait, the state is periodic.

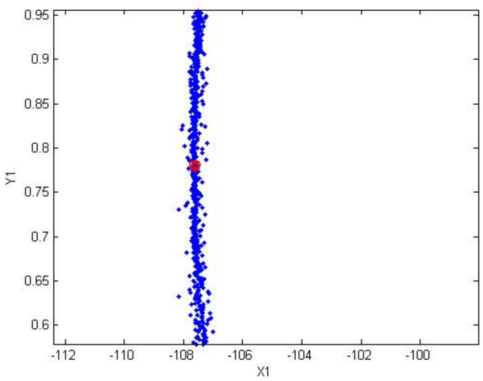


Fig. 4.9 (c) It is the magnified diagram of Fig.4.9 (a).

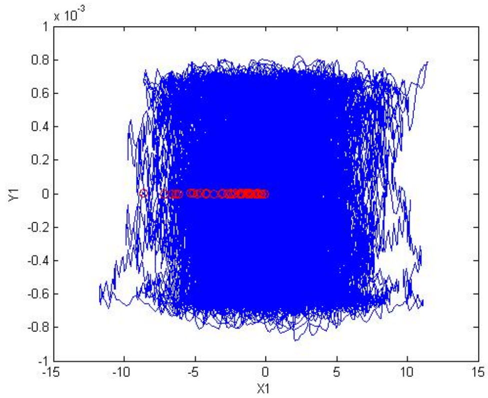


Fig. 4.10 The phase portrait, the delay time $\tau_2$ of system (4.1) is replaced by $200+0.612x_2$.

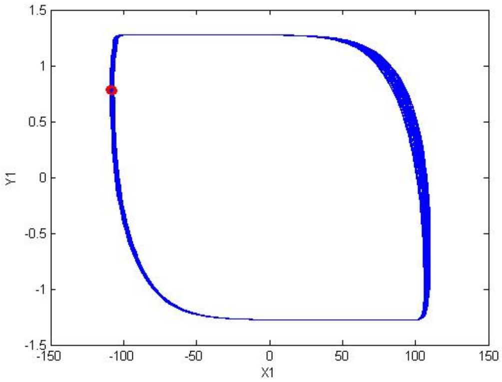


Fig. 4.11 (a) The phase portrait, the delay time $\tau_1$ of system (4.1) is replaced by $200+0.1y_2$.

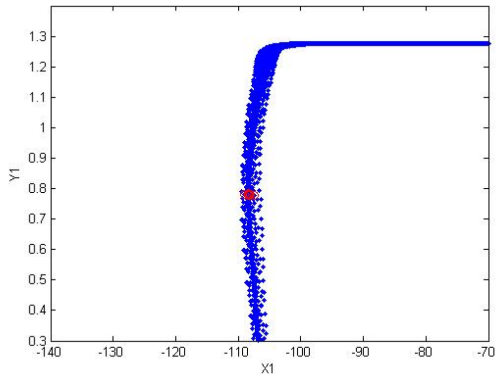


Fig. 4.11 (b) It is the magnified diagram of Fig.4.11 (a).

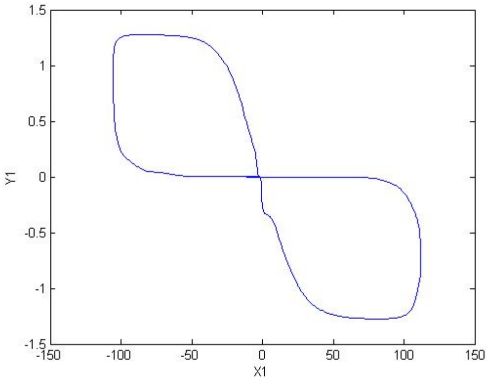


Fig. 4.12 The phase portrait, the delay time $\tau_2$ of system (4.1) is replaced by $200+0.1y_2$.

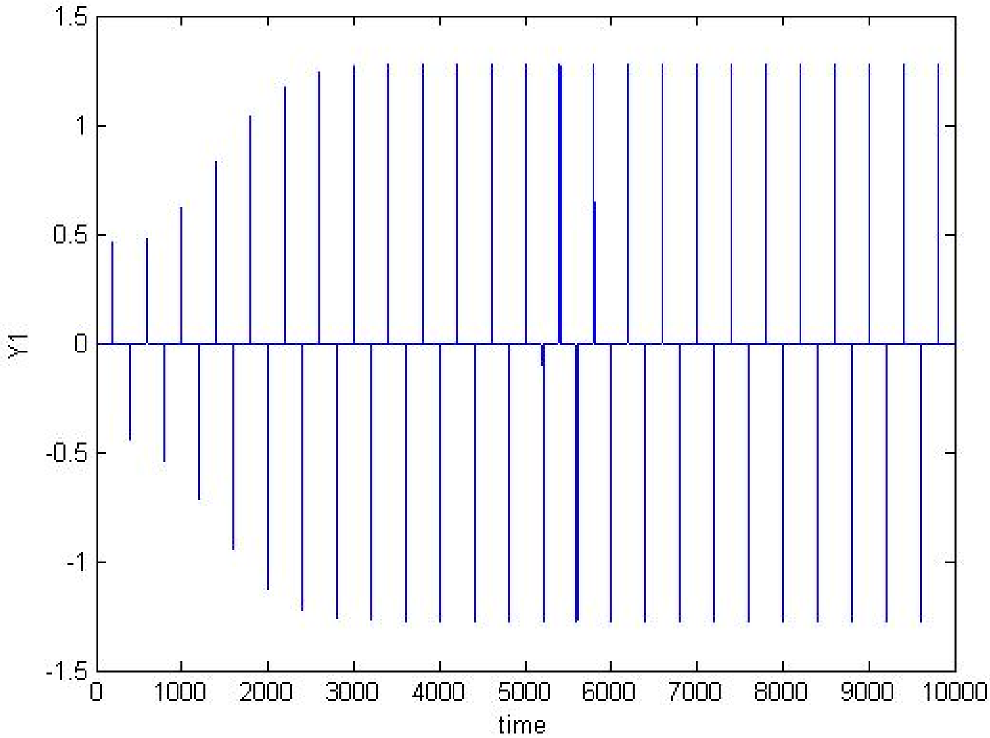


Fig. 4.13 The time history, the delay time $\tau_2$ of system (4.1) is replaced by $200+0.1y_2$.

# Chapter 5

# Robust Lag Chaos Synchronization, Lag Chaos Quasi-Synchronization and Chaos Control of Double Ikeda System by Uncoupled Parameter Excited Method

## 5.1 Preliminaries

In this chapter, lag synchronization, lag quasi-synchronization and chaos control of two uncoupled double Ikeda systems, are achieved by replacing the corresponding parameters of two systems by the chaotic state variables of a third chaotic system. It is named as parameter excited method for synchronization. Numerical simulations are illustrated by phase portraits, Poincaré maps and time histories.

## 5.2 Lag Chaos Synchronization, Lag Chaos Quasi-Synchronization and Chaos Control with Parameters Replaced by Different Chaotic Signals

In this section, consider three identical double Ikeda systems：

$$\begin{cases} \dot{x}_1 = -a_1 x_1 - b_1 \sin x_{1\tau_1} - c \sin y_1 \\ \dot{y}_1 = -a_2 y_1 - b_2 \sin y_{1\tau_2} \end{cases} \tag{5.1}$$

and

$$\begin{cases} \dot{x}_2 = -a_1 x_2 - b_1 \sin x_{2\tau_1} - c \sin y_2 \\ \dot{y}_2 = -a_2 y_2 - b_2 \sin y_{2\tau_2} \end{cases} \tag{5.2}$$

and

$$\begin{cases} \dot{x}_3 = -a_1 x_3 - b_1 \sin x_{3\tau_1} - c \sin y_3 \\ \dot{y}_3 = -a_2 y_3 - b_2 \sin y_{3\tau_2} \end{cases} \tag{5.3}$$

The scheme is to replace the parameters $b_1$, $b_2$ in system (5.1) and (5.2) by two different chaotic states of system (5.3), respectively. One replaces a parameter in system (5.1) by a chaotic state of system (5.3), and replaces the corresponding parameter in system (5.2) by the same chaotic state of system (5.3) with a delay time $\tau_3$.

In following simulations, the parameter in system (5.1) is replaced by $x_3$ where $x_3$ is a state variable in system (5.3). The parameter in system (5.2) is replaced by $x_3(t-\tau_3) = x_{3_{\tau_3}}$ where $\tau_3$ is a constant. In our numerical simulations, $a_1 = 1$, $a_2 = 15$, $b_1 = 20$, $b_2 = 20$, $c = 157$, $\tau_1 = \tau_2 = 2s$ of system (5.1), (5.2) and (5.3) are fixed. The initial states of system (5.1), (5.2) and (5.3) are $x_1(0) = -1$, $y_1(0) = -1$, $x_2(0) = -1.1$, $y_2(0) = -1.1$, $x_3(0) = -1$, $y_3(0) = -1$. Chaotic phase portraits are shown in Fig. 5.1. The numerical simulations are carried out by MATLAB.

The parameter $b_1$ of system (5.1) is replaced by $x_3$, and the parameter $b_1$ of system (5.2) is replaced by $x_{3_{\tau_3}}$. $\tau_3$=10, 50, 100 are used in simulation. The phase portraits, Poincaré maps and time histories are shown in Figs. 5.2~5.4. Fig.5.3 (d) is the magnified diagram of Fig.5.3 (b). Fig.5.3 (e) is the magnified diagram of Fig.5.3 (c). Fig.5.4 (d) is the magnified diagram of Fig.5.4 (b). Fig.5.4 (e) is the magnified diagram of Fig.5.4 (c).

In these cases, we can find the lag quasi-synchronization between $x_1$ and $x_2$, and lag synchronization between $y_1$ and $y_2$.

Then the parameter $b_2$ of system (5.1) is replaced by $y_3$, and the parameter $b_2$ of system (5.2) is replaced by $y_{3_{\tau_3}}$, where $\tau_3$=100. The phase portraits are shown in Fig. 5.5. In this case, by parameter excited method we successfully control $x_1$, $x_2$ to constants, and $y_1$, $y_2$ to zero.

Parameter excited method for lag synchronization by replacements of $a_1$, $a_2$ and c has not been found effective.

## 5.3 Robustness of Lag Chaos Synchronization

In the section, noises are added to systems (5.1) and (5.2) as follows :

$$\begin{cases} \dot{x}_1 = -a_1 x_1 - b_1 \sin x_{1_{\tau_1}} - c \sin y_1 + kN_1 \\ \dot{y}_1 = -a_2 y_1 - b_2 \sin y_{1_{\tau_2}} \end{cases} \tag{5.4}$$

and

$$\begin{cases} \dot{x}_2 = -a_1 x_2 - b_1 \sin x_{2_{\tau_1}} - c \sin y_2 + kN_2 \\ \dot{y}_2 = -a_2 y_2 - b_2 \sin y_{2_{\tau_2}} \end{cases} \tag{5.5}$$

where k is strength constant, and $N_1, N_2$ are different kinds of noise.

Three kind of noise are used. There are Gaussian noise, Rayleigh noise, and Rician noise.

The probability density function of n-dimensional Gaussian noise is

$$f(x) = ((2\pi)^n \det K)^{-\frac{1}{2}} \exp(-(x-\mu)^T K^{-1}(x-\mu)/2) \tag{5.6}$$

where $x$ is a length-n vector, $K$ is the n-by-n covariance matrix, $\mu$ is the mean value vector, and the superscript $T$ indicates matrix transpose. The Simulink Communications toolbox provides the Gaussian Noise Generator block. The initial seed, the mean value and the variance in the simulation must be specified. We take the initial seed 41, the mean value 1 and the variance 1 in the simulation.

The Rayleigh probability density function is given by

$$f(x)=\begin{cases}\dfrac{x}{\sigma^2}e^{-\frac{x^2}{2\sigma^2}} & x\ge 0\\ 0 & x<0\end{cases} \tag{5.7}$$

where $\sigma^2$ is known as the fading envelope of the Rayleigh distribution. The Simulink Communications toolbox provides the Rayleigh Noise Generator block. The initial seed and the sigma parameter in the simulation must be specified. We specify the initial seed 47 and the sigma parameter 1 in the simulation.

The Rician probability density function is given by

$$f(x)=\begin{cases}\dfrac{x}{\sigma^2}I_0\left(\dfrac{mx}{\sigma^2}\right)e^{-\frac{x^2+m^2}{2\sigma^2}} & x\ge 0\\ 0 & x<0\end{cases} \tag{5.8}$$

where $\sigma$ is the standard deviation of the Gaussian distribution that underlies the Rician distribution noise, $m^2=m_I^2+m_Q^2$, where $m_I$ and $m_Q$ are the mean values of two independent Gaussian components, and $I_0$ is the modified 0th-order Bessel function of the first kind given by

$$I_0(y)=\frac{1}{2\pi}\int_{-\pi}^{\pi}e^{y\cos t}dt \tag{5.9}$$

Note that $m$ and $\sigma$ are not the mean value and standard deviation for the Rician noise. The Simulink Communications toolbox provides the Rician Noise Generator block. The initial seed, Rician K-factor and the sigma parameter must be specified in the simulation. We specify the initial seed 59, Rician K-factor 2 and the sigma parameter 1 in the simulation.

External terms $kN_1$, $kN_2$ are added to systems of (5.4) and (5.5), where $N_1$,

$N_2$ are the Gaussian noise and Rayleigh noise, respectively. In addition, the parameter $b_1$ of system (5.4) is replaced by $x_3$, and the parameter $b_1$ of system (5.5) by $x_{3_{\tau_3}}$ where $\tau_3$=10. k=1, k=50 are used. For k=1, as shown in Fig. 5.6, robustness of lag synchronization of $y_1$, $y_2$ and of lag quasi-synchronization of $x_1$, $x_2$ is satisfactory. For k=50, as shown in Fig. 5.7, robustness of lag synchronization of $y_1$, $y_2$ is still satisfactory, but robustness of the lag quasi-synchronization of $x_1$, $x_2$ is lost.

Lastly, external terms $kN_1$, $kN_2$ are added to the systems of (5.4) and (5.5), where $N_1$, $N_2$ are the Gaussian noise and Rician noise, respectively. The parameter $b_1$ of system (5.4) is replaced by $x_3$, and the parameter $b_1$ of system (5.5) by $x_{3_{\tau_3}}$ where $\tau_3$=10. k=1, k=30 are used. For k=1, as shown in Fig. 5.8, robustness of lag synchronization of $y_1$, $y_2$ and of lag quasi-synchronization of $x_1$, $x_2$ is satisfactory. For k=30, as shown in Fig. 5.9, robustness of lag synchronization of $y_1$, $y_2$ is still satisfactory, but robustness of the lag quasi-synchronization of $x_1$, $x_2$ is lost.

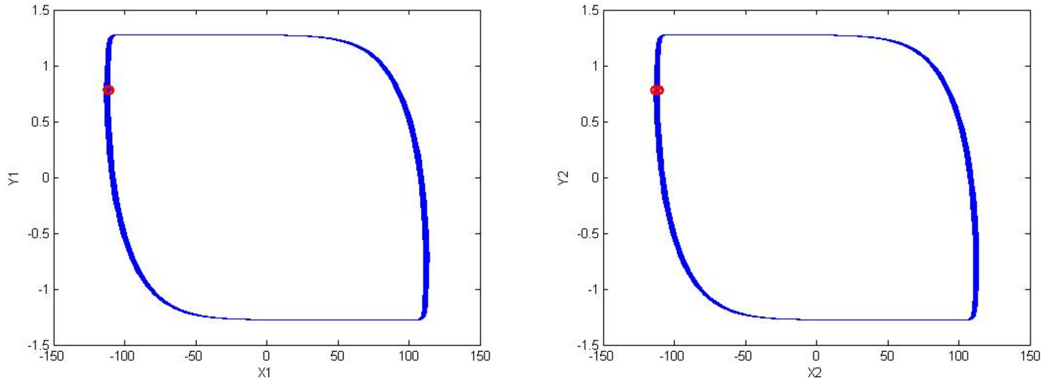


Fig. 5.1 The phase portraits for systems (5.1) and (5.2).

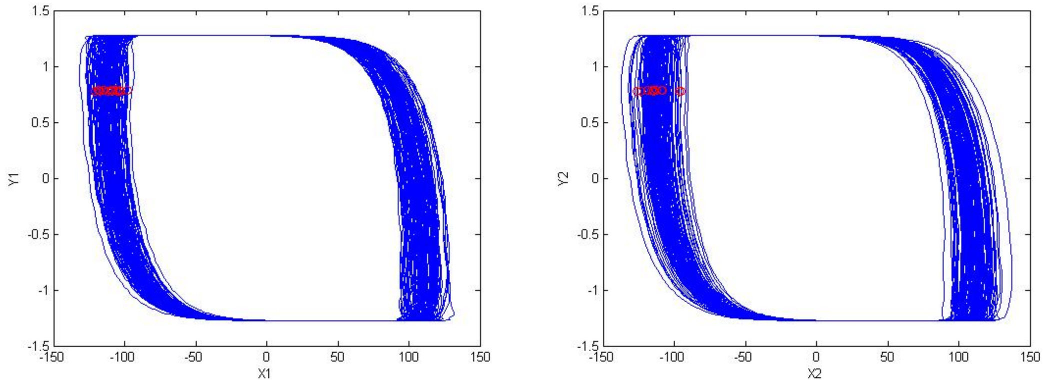


(a)

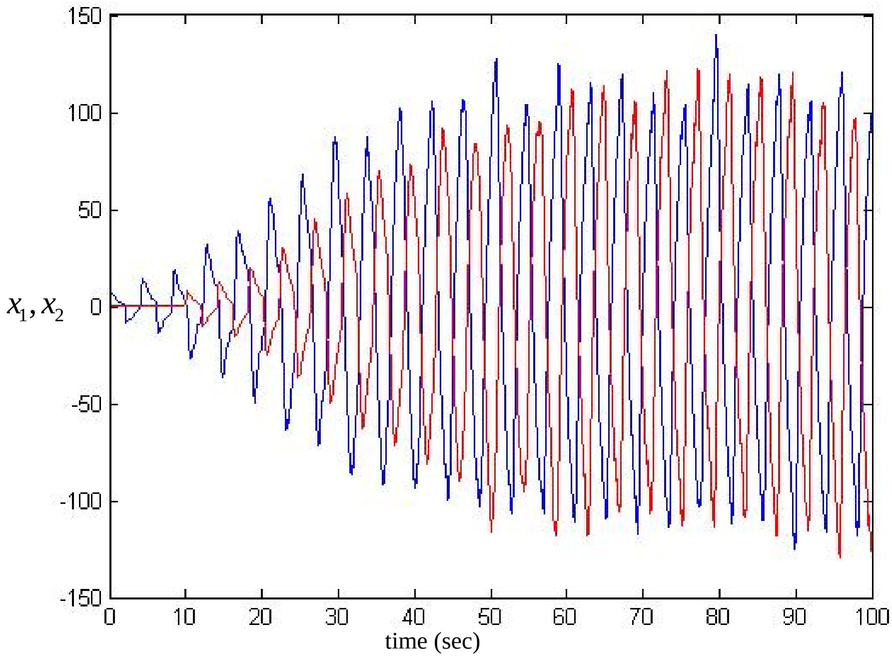


(b)

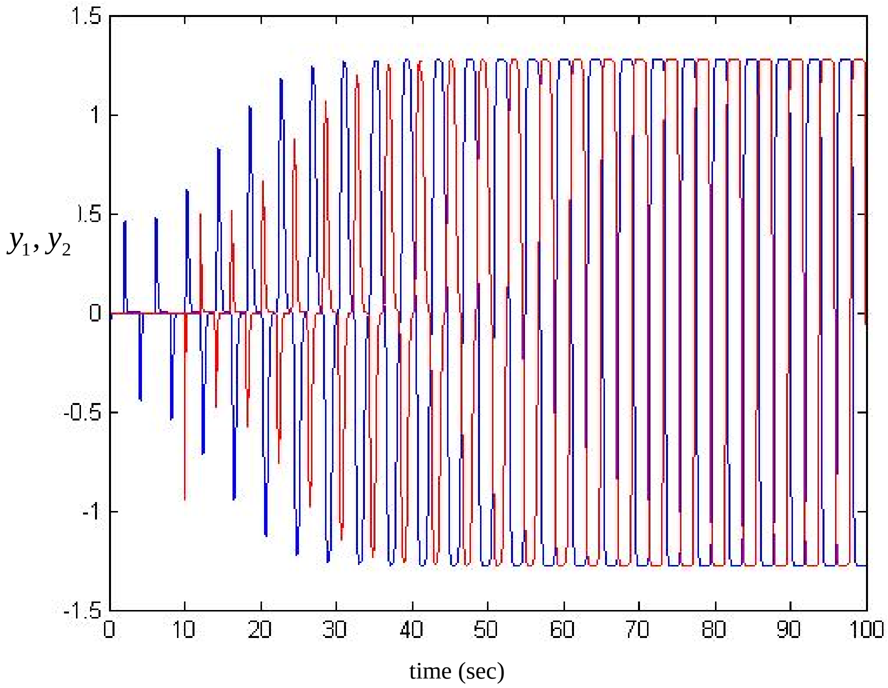


(c)

Fig. 5.2 (a) The phase portraits, $\tau_3$=10. (b) The time histories of $x_1$ (blue) and $x_2$ (red), $\tau_3$=10. (c) The time histories of $y_1$ (blue) and $y_2$ (red), $\tau_3$=10.

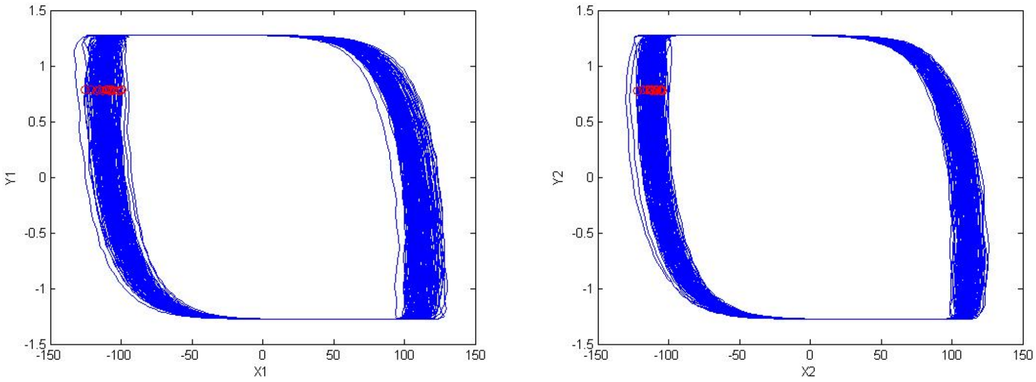


(a)

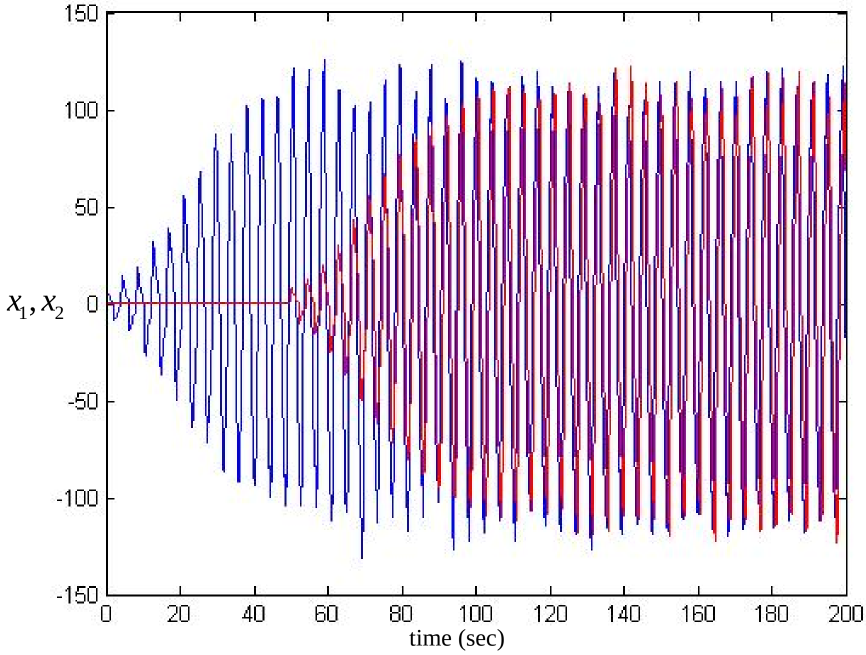


(b)

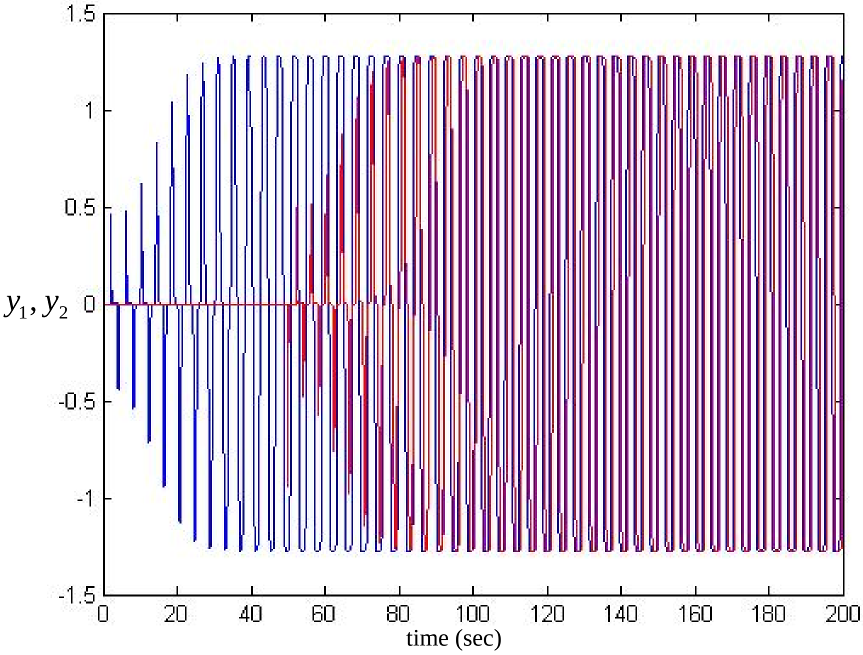

1.5
1
0.5
$y_1, y_2$ 0
-0.5
-1
-1.5
0 20 40 60 80 100 120 140 160 180 200
time (sec)


(c)

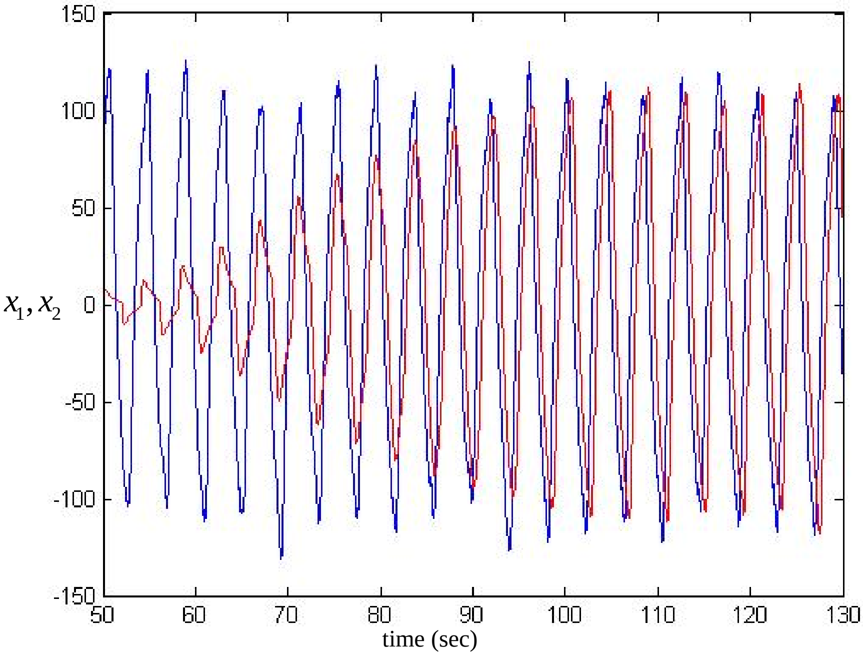

150
100
50
$x_1, x_2$ 0
-50
-100
-150
50 60 70 80 90 100 110 120 130
time (sec)


(d)

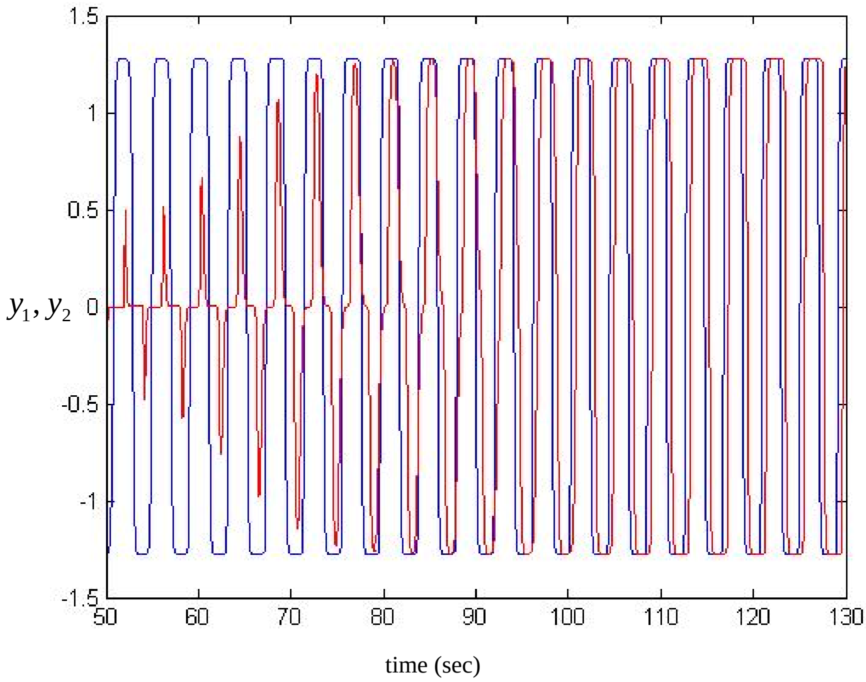


(e)

Fig. 5.3 (a) The phase portraits, $\tau_3$=50. (b) The time histories of $x_1$ (blue) and $x_2$ (red), $\tau_3$=50. (c) The time histories of $y_1$ (blue) and $y_2$ (red), $\tau_3$=50. (d) Magnified diagram of (b). (e) Magnified diagram of (c).

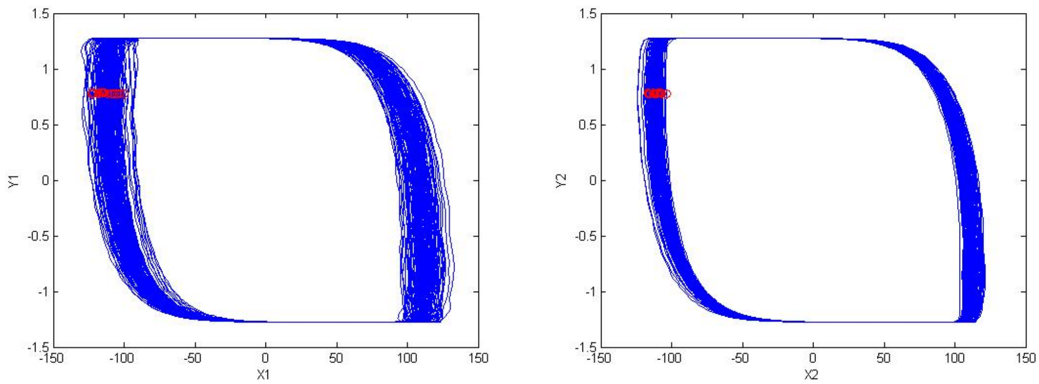


(a)

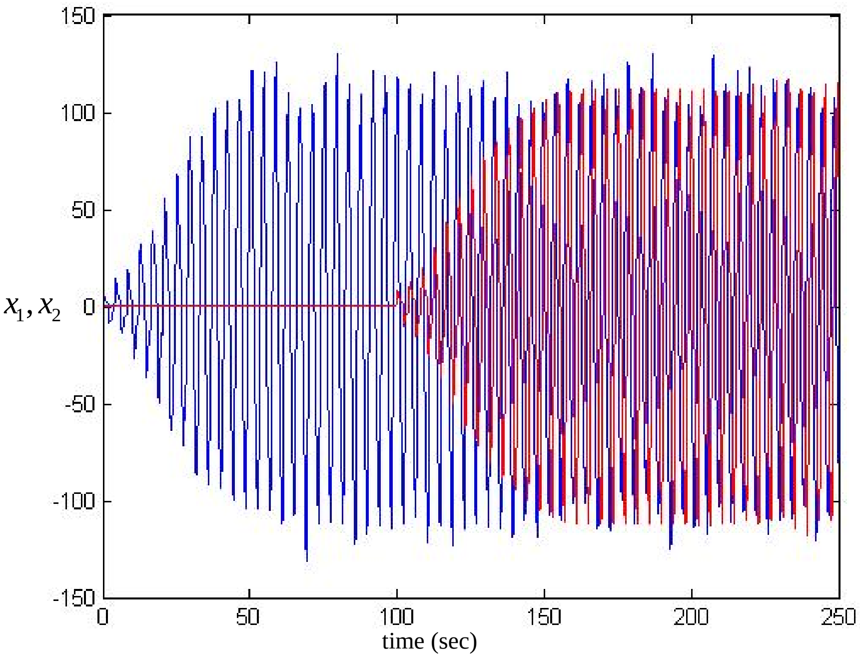
150
100
50
$x_1, x_2$ 0
-50
-100
-150
0
50
100
150
200
250
time (sec)

(b)

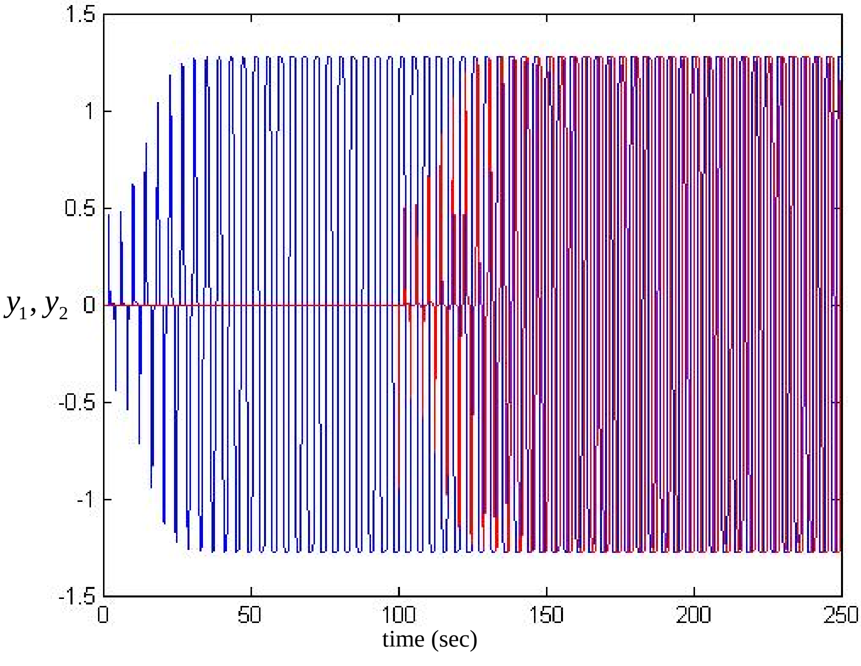
1.5
1
0.5
$y_1, y_2$ 0
-0.5
-1
-1.5
0
50
100
150
200
250
time (sec)

(c)

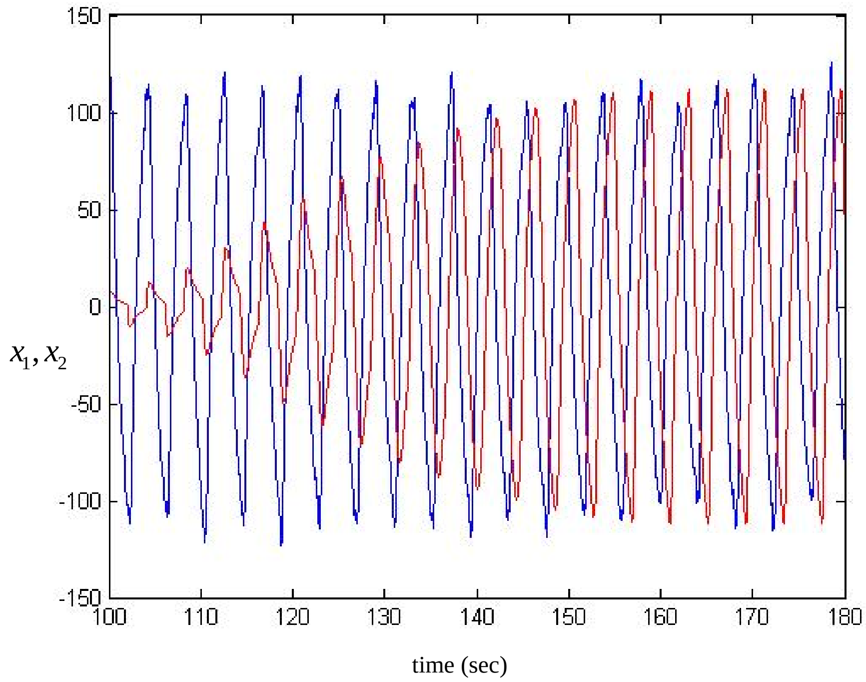


(d)

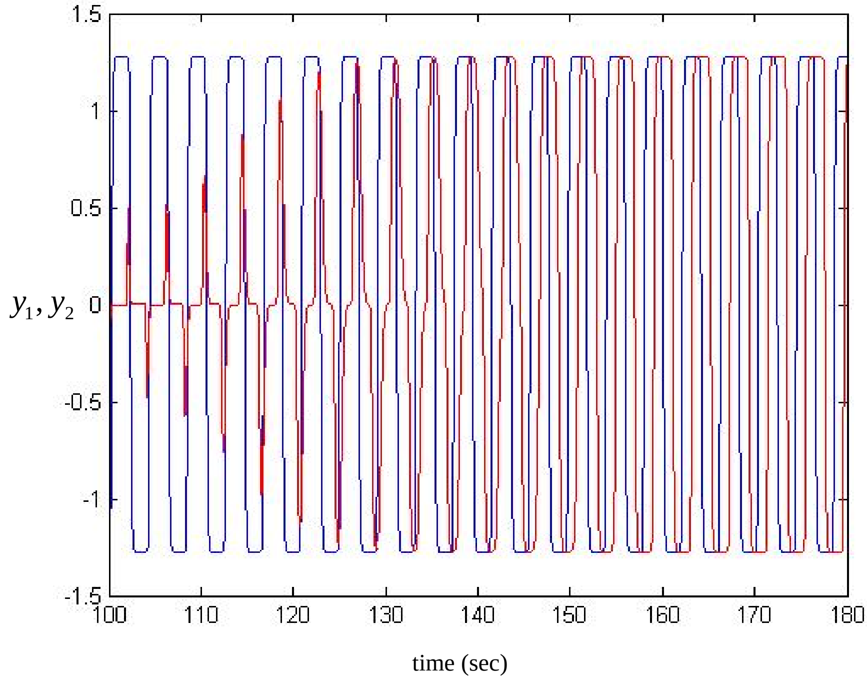


(e)

Fig. 5.4 (a) The phase portraits, $\tau_3$=100. (b) The time histories of $x_1$ (blue) and $x_2$ (red), $\tau_3$=100. (c) The time histories of $y_1$ (blue) and $y_2$ (red), $\tau_3$=100. (d) Magnified diagram of (b). (e) Magnified diagram of (c).

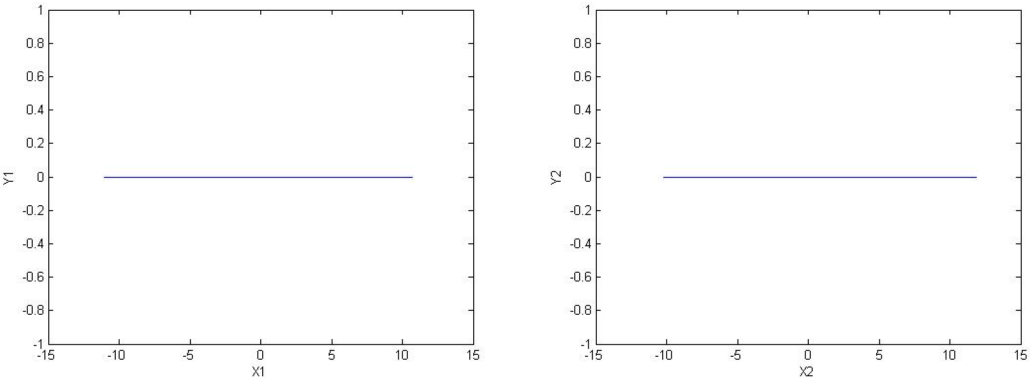


Fig. 5.5 The phase portraits, $\tau_3$=100.

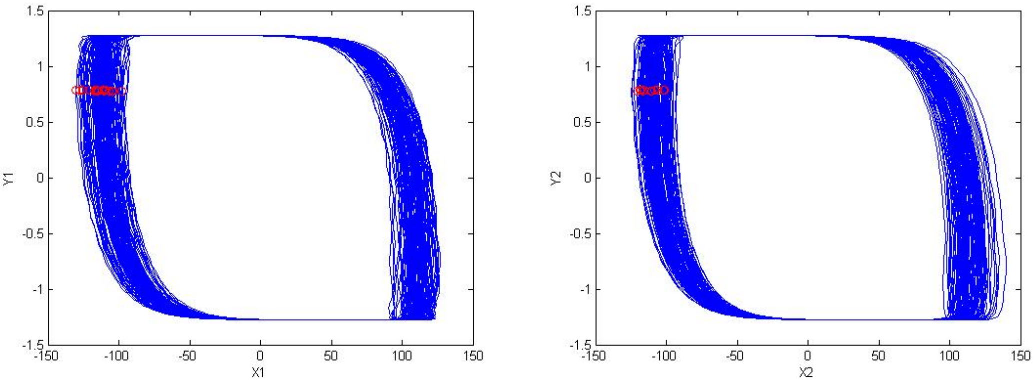


(a)

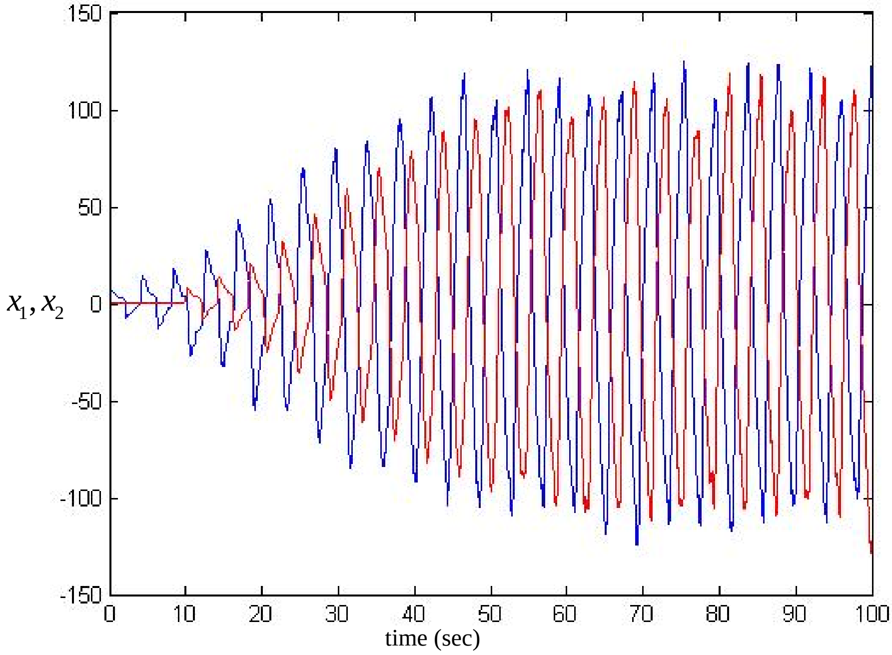

(b)

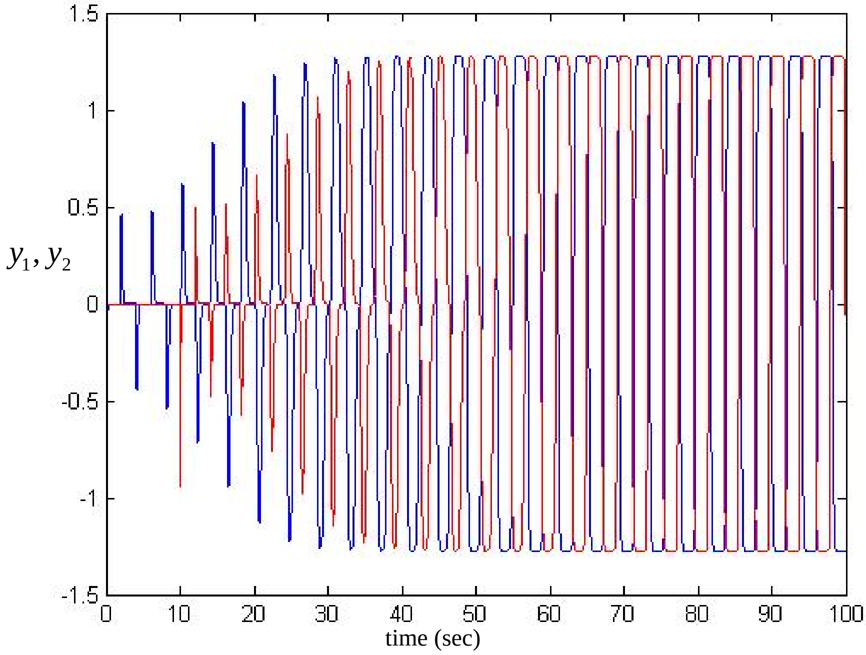


(c)

Fig. 5.6 (a) The phase portraits, $\tau_3$=10 and k=1. (b) The time histories of $x_1$ (blue) and $x_2$ (red), $\tau_3$=10 and k=1. (c) The time histories of $y_1$ (blue) and $y_2$ (red), $\tau_3$=10 and k=1.

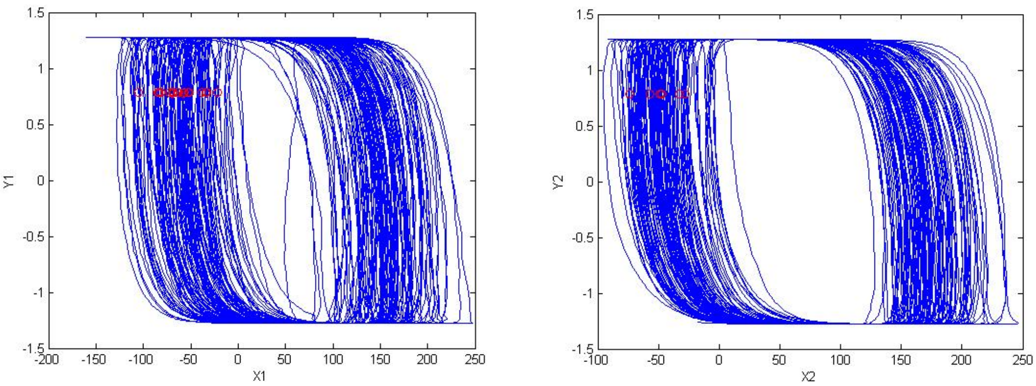


(a)

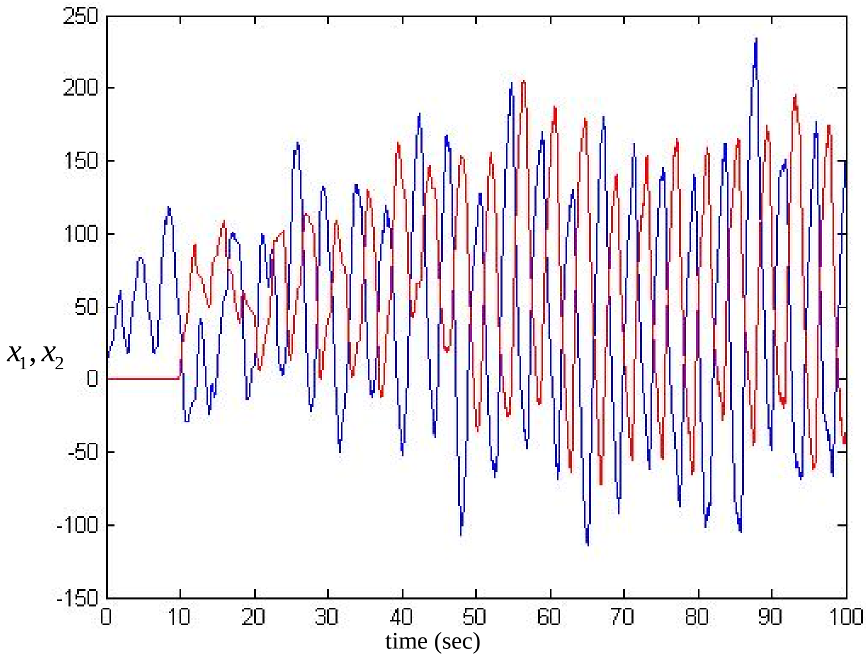


(b)

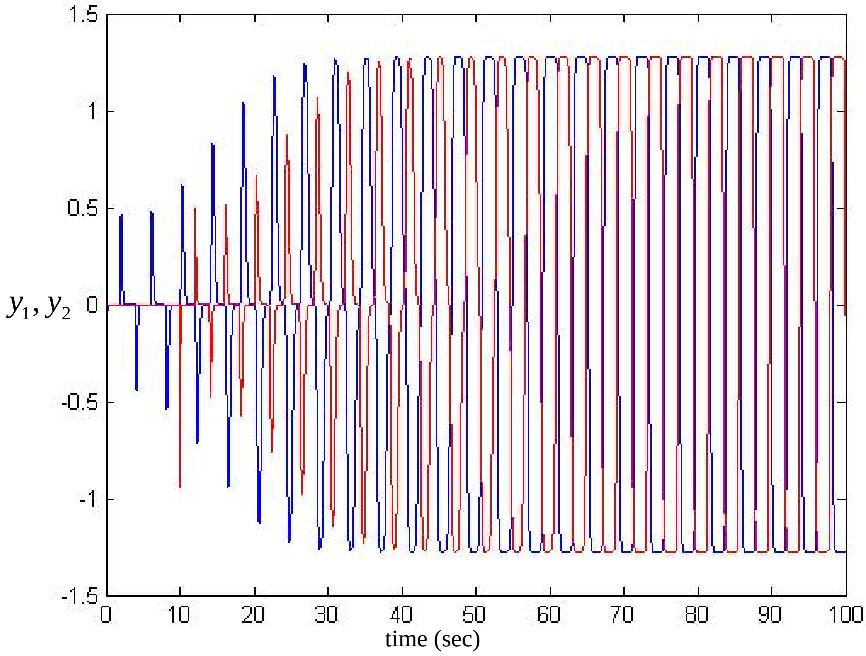


(c)

Fig. 5.7 (a) The phase portraits, $\tau_3$=10 and k=50. (b) The time histories of $x_1$ (blue) and $x_2$ (red), $\tau_3$=10 and k=50. (c) The time histories of $y_1$ (blue) and $y_2$ (red), $\tau_3$=10 and k=50.

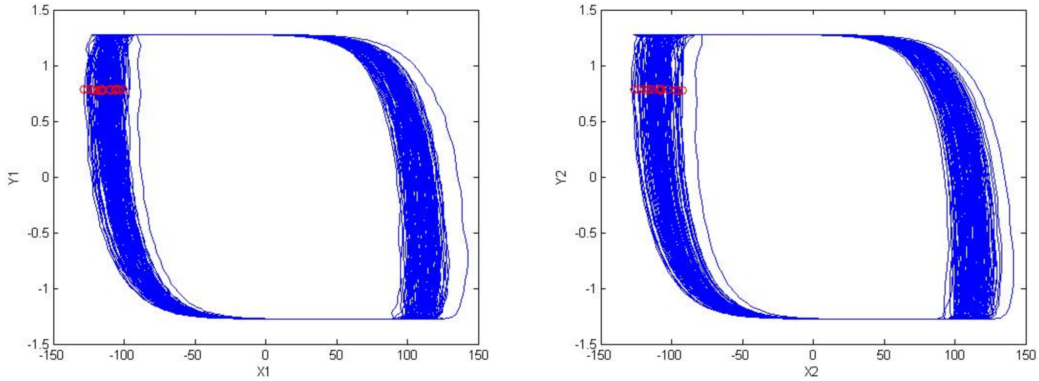


(a)

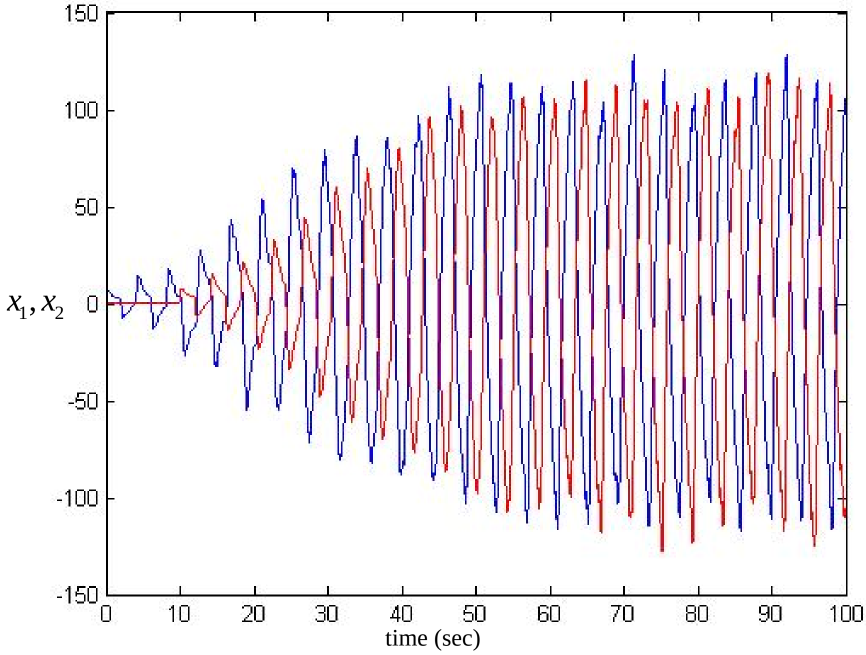


(b)

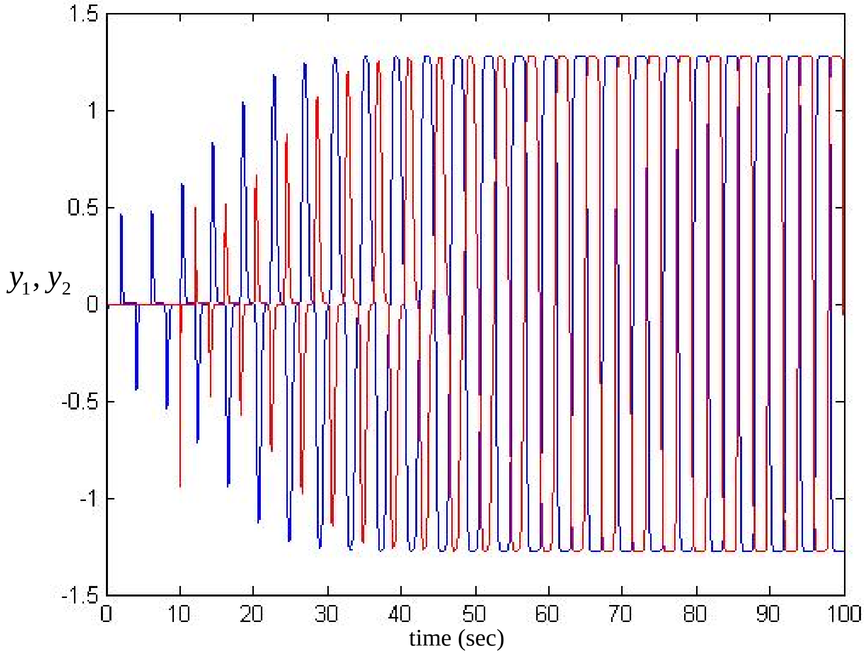


(c)

Fig. 5.8 (a) The phase portraits, $\tau_3$=10 and k=1. (b) The time histories of $x_1$ (blue) and $x_2$ (red), $\tau_3$=10 and k=1. (c) The time histories of $y_1$ (blue) and $y_2$ (red), $\tau_3$=10 and k=1.

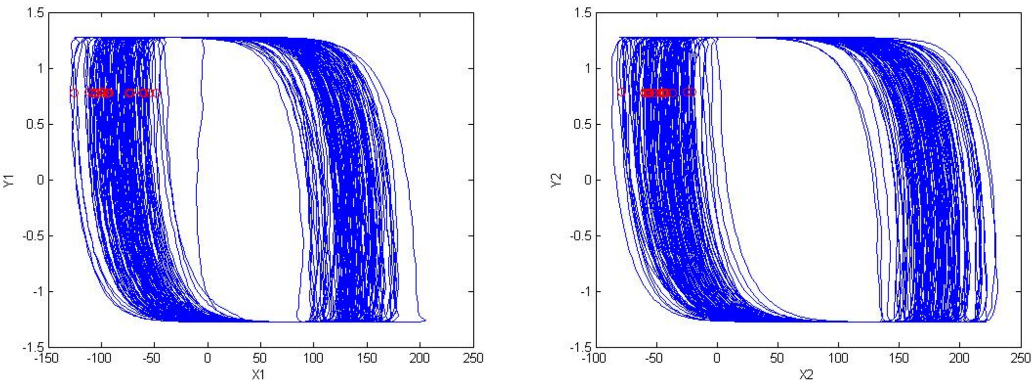


(a)

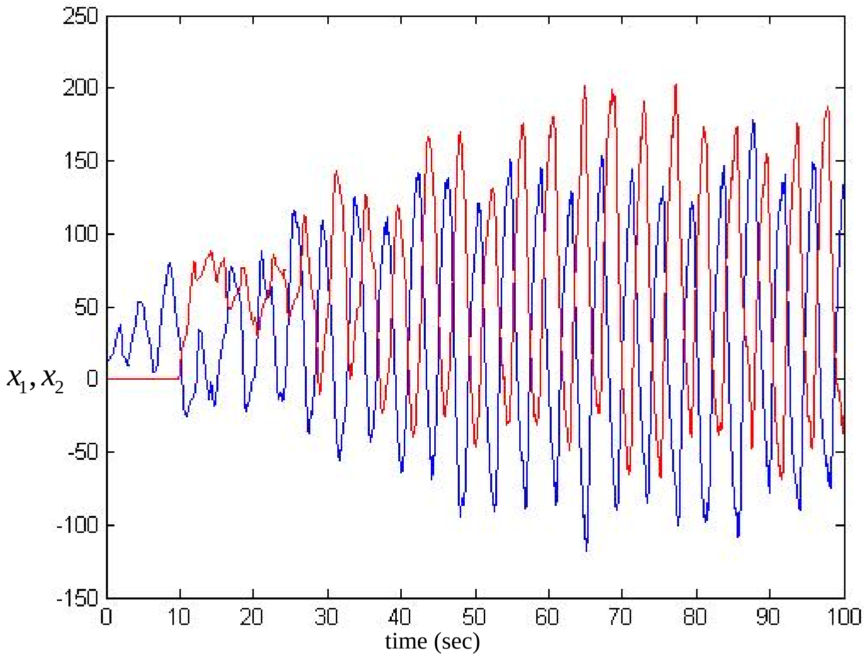


(b)

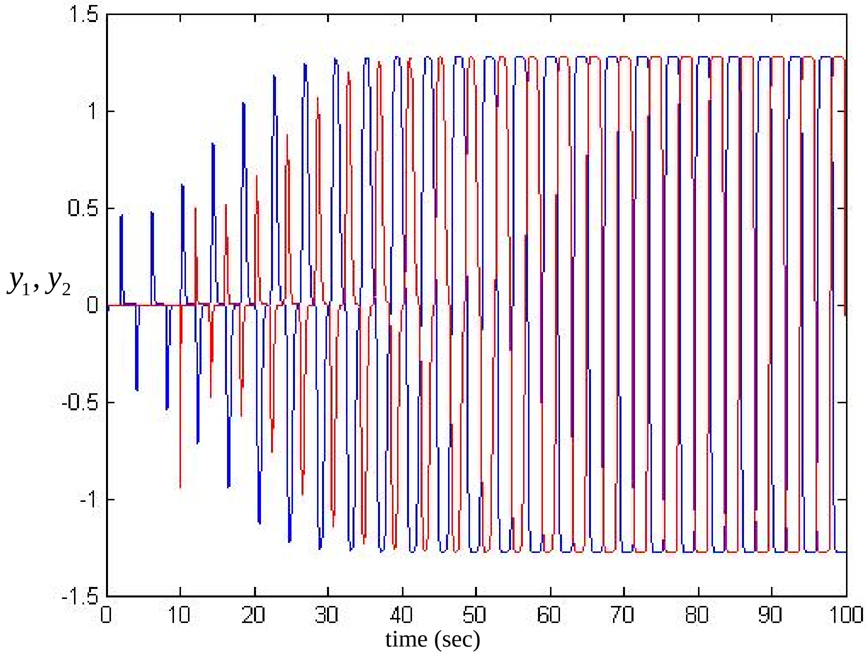


(c)

Fig. 5.9 (a) The phase portraits, $\tau_3$=10 and k=30. (b) The time histories of $x_1$ (blue) and $x_2$ (red), $\tau_3$=10 and k=30. (c) The time histories of $y_1$ (blue) and $y_2$ (red), $\tau_3$=10 and k=30.

# Chapter 6

# Conclusions

In this thesis, we have studied the chaos in the integral and fractional order double Ikeda systems by phase portraits, Poincaré maps and bifurcation diagrams. In Chapter 2, the chaos in integral and fractional order double Ikeda systems with total order of derivatives from 2 to 0.2 are studied by phase portraits, Poincaré maps and bifurcation diagrams. It is found that chaos exists in all cases.

In Chapter 3, lag or anticipated synchronization and the lag or anticipated anti-synchronization of two double Ikeda systems with different initial conditions are discovered. Cases 1~8 are the lag or anticipated synchronizations. Cases 9~16 are the lag or anticipated anti-synchronizations.

In Chapter 4, the chaotic behaviors of double Ikeda systems are obtained by replacing their delay time by a function of chaotic state variables of a second chaotic system. It is found that chaos exists for Case 1, 3, 5, 6. The chaotization of a double Ikeda system is studied by using a function of state variable of a second identical system to replace the delay time of the first system. It is found that in Case 7, 8, 9, chaotization exists.

In Chapter 5, robust lag chaos synchronization, lag quasi-synchronization and chaos control of two uncoupled double Ikeda system, are achieved by replacing the corresponding parameters of two systems by different chaotic state variables of a third chaotic system. Robustness of synchronization is studied by addition of various noises. The results are satisfactory.

# References

[1] Koliopanos, Ch.L.; Kyprianidis, I.M.; Stouboulos, I.N.; Anagnostopoulos, A.N.; Magafas, L. “Chaotic behaviour of a fourth-order autonomous electric circuit”. Chaos, Solitons & Fractals 2003;16:173-82.

[2] Lu, Jun Guo “Synchronization of a class of fractional-order chaotic systems via a scalar transmitted signal”. Chaos, Solitons & Fractals 2006;27:519-25.

[3] Lu, Jun Guo “Chaotic dynamics and synchronization of fractional-order Arneodo_s systems”. Chaos, Solitons & Fractals 2005;26:1125-33.

[4] Gao, Xin; Yu, Juebang “Synchronization of two coupled fractional-order chaotic oscillators”. Chaos, Solitons & Fractals 2005;26:141-5.

[5] Ge, Zheng-Ming; Lee, Ching-I “Control, anticontrol and synchronization of chaos for an autonomous rotational machine system with time-delay”. Chaos, Solitons & Fractals 2005;23:1855-64.

[6] Ge, Zheng-Ming; Chen, Yen-Sheng “Adaptive synchronization of unidirectional and mutual coupled chaotic systems”. Chaos, Solitons & Fractals 2005;26:881-8.

[7] Ge, Zheng-Ming; Chen, Yen-Sheng “Synchronization of unidirectional coupled chaotic systems via partial stability”. Chaos, Solitons & Fractals 2004;21:101-11.

[8] Ge, Zheng-Ming; Chen, Chien-Cheng “Phase synchronization of coupled chaotic multiple time scales systems”. Chaos, Solitons & Fractals 2004;20:639-47.

[9] Ge, Zheng-Ming; Lee, Ching-I “Anticontrol and synchronization of chaos for an autonomous rotational machine system with a hexagonal centrifugal governor”. Journal of Sound and Vibration 2005;282:635-48.

[10] Zheng-Ming Ge, Chan-Yi Ou "Chaos in a fractional order modified Duffing

system", Chaos, Solitons and Fractals, in press.

[11] Zheng-Ming Ge, Chang-Xian Yi "  Chaos in a nonlinear damped Mathieu System, in a nano Resonator system and in its fractional order systems", Solitons and Fractals, in press.

[12] Zheng-Ming Ge, Mao-Yuan Hsu "  Chaos in a generalized van der Pol system and in its fractional order system", Chaos, Solitons and Fractals, in press.

[13] Zheng-Ming Ge, An-Ray Zhang "Chaos in a modified van der Pol system and in its fractional order systems", Chaos, Solitons and Fractals, in press.

[14] Ahmad, Wajdi M. “Generation and control of multi-scroll chaotic attractors in fractional order systems”. Chaos, Solitons & Fractals 2005;25:727-35.

[15] Gao, Xin; Yu, Juebang “Chaos in the fractional order periodically forced complex Duffing_s oscillators”. Chaos, Solitons & Fractals 2005;24: 1097-104.

[16] Ahmad, Wajdi M.; Harb, Ahmad M. “On nonlinear control design for autonomous chaotic systems of integer and fractional orders”. Chaos, Solitons & Fractals 2003;18:693-701.

[17] Nimmo, Stuart; Evans, Allan K. “The Effects of Continuously Varying the Fractional Differential Order of Chaotic Nonlinear Systems”. Chaos, Solitons & Fractals 1999;10:1111-8.

[18] J. M. Ottino et al., “Chaos, Symmetry, and Self-Similarity: Exploiting Order and Disorder in Mixing Process”, Science, Vol. 257, pp. 754-760(1992).

[19] S. J. Schiff, K. Jerger, D. H. Duong, T. Chang, M. L. Spano, and W. L. Ditto, “Controlling Chaos in the Brain”, Nature, Vol. 370, pp. 615-620(1994).

[20] M. E. Brandt and G. Chen, “Bifurcation Control of Two Nonlinear Models of Cardiac Activity”, IEEE Trans. Circuits Syst., Vol. 44, pp. 1031-1034(1997).

[21] Al-Assaf, Yousef; El-Khazali, Reyad; Ahmad, Wajdi “Identification of fractional chaotic system parameters”. Chaos, Solitons & Fractals 2004;22:897-905.

[22] Ahmad, Wajdi M.; El-Khazali, Reyad; Al-Assaf, Yousef pp. “Stabilization of generalized fractional order chaotic systems using state feedback control”. Chaos, Solitons & Fractals 2004;22:141-50.

[23] He, G.L.; Zhou, S.P. “What is the exact condition for fractional integrals and derivatives of Besicovitch functions to have exact box dimension?” Chaos, Solitons & Fractals 2005;26:867-79.

[24] Yao, K.; Su, W.Y.; Zhou, S.P. “On the connection between the order of fractional calculus and the dimensions of a fractal function”. Chaos, Solitons & Fractals 2005;23: 621-9.

[25] Jumarie, Guy “Fractional master equation: non-standard analysis and Liouville–Riemann derivative”. Chaos, Solitons & Fractals 2001;12: 2577-87.

[26] Elwakil, S. A.; Zahran, M. A. “Fractional Integral Representation of Master Equation”. Chaos, Solitons & Fractals 1999;10: 1545-8.

[27] Podlubny I. “Fractional differential equations”. New York: Academic Press; 1999.

[28] Hilfer R, editor. “Applications of fractional calculus in physics”. New Jersey: World Scientific; 2001.

[29] Bagley RL, Calico RA. “Fractional order state equations for the control of viscoelastically damped structures”. J Guid Contr Dyn 1991;14:304–11.

[30] Sun HH, Abdelwahad AA, Onaral B. “Linear approximation of transfer function with a pole of fractional order”. IEEE Trans Automat Contr 1984;29:441–4.

[31] Ichise M, Nagayanagi Y, Kojima T. “An analog simulation of noninteger order transfer functions for analysis of electrode process”. J Electroanal Chem 1971;33:253–65.

[32] Heaviside O. “Electromagnetic theory”. New York: Chelsea; 1971.

[33] Laskin N. “Fractional market dynamics”. Physica A 2000;287:482–92.

[34] Kusnezov D, Bulgac A, Dang GD. "Quantum levy processes and fractional kinetics". Phys Rev Lett 1999;82:1136–9.

[35] Pecora, L.M. and Carroll, T.L., "Synchronization in chaotic systems",Phys. Rev. Lett. 64:821–4;1990.

[36] Chen H.-K. "Synchronization of two different chaotic systems: a new system and each of the dynamical systems Lorenz, Chen and Lü", Chaos, Solitons and Fractals Vol. 25; 1049-56, 2005.

[37] Chen H.-K. and Lin T.-N. "Synchronization of chaotic symmetric gyros by one-way coupling conditions", ImechE Part C: Journal of Mechanical Engineering Science Vol. 217; 331-40, 2003.

[38] Chen H.-K. "Chaos and chaos synchronization of a symmetric gyro with linear-plus-cubic damping", Journal of Sound & Vibration, Vol. 255; 719-40,2002.

[39] Ge Z.-M., Yu T.-C., and Chen Y.-S. "Chaos synchronization of a horizontal platform system", Journal of Sound and Vibration 731-49, 2003.

[40] Ge Z.-M. and Lin T.-N. "Chaos, chaos control and synchronization of electro-mechanical gyrostat system", Journal of Sound and Vibration Vol. 259; No.3, 2003.

[41] Ge Z.-M., Lin C.-C. and Chen Y.-S. "Chaos, chaos control and synchronization of vibromrter system", Journal of Mechanical Engineering Science Vol. 218; 1001-20, 2004.

[42] Awad El-Gohary and Rizk Yassen "Adaptive control and synchronization of a coupled dynamo system with uncertain parameters"

[43] Yang Y., Ma X.-K and Zhang H. "Synchronization and parameter identification of high-dimensional discrete chaotic systems via parametric adaptive control", Chaos, Solitons and Fractals 28; 244-251, 2006.

[44] Ge Z.-M., Tzen P.-C. and LeeS.-C. "Parametric analysis and fractal-like basins of attraction by modified interpolates cell mapping", Journal of Sound and Vibration Vol. 253; No. 3, 2002.

[45] Ge Z.-M. and Lee S.-C. "Parameter used and accuracies obtain in MICM global analyses", Journal of Sound and Vibration Vol. 272; 1079-85, 2004.

[46] Ge Z.-M. and Leu W.-Y. "Chaos synchronization and parameter identification for loudspeaker system" Chaos, Solitons and Fractals Vol. 21; 1231-47, 2004.

[47] Ge Z.-M. and Chang C.-M. "Chaos synchronization and parameter identification for single time scale brushless DC motor", Chaos, Solitons and Fractals Vol. 20; 889-903, 2004.

[48] Ge Z.-M. and Lee J.-K. "Chaos synchronization and parameter identification for gyroscope system", Applied Mathematics and Computation, Vol. 63; 667-82, 2004.

[49] Ge Z.-M. and Cheng J.-W. "Chaos synchronization and parameter identification of three time scales brushless DC motor", Chaos, Solitons and Fractals Vol. 24; 597-616, 2005.

[50] Edouard, D., Dufour, P. and Hammouri, H. "Observer based multivariable control of a catalytic reverse flow reactor: comparison between LQR and MPC approaches ", Computers and Chemical Engineering 29; 851-865, 2005.

[51] Ho H.-F., Wong Y.-K., Rad A.-B. and Lo W.-L. "State observer based indirect adaptive fuzzy tracking control", Simulation Modelling Practice and Theory 13; 646-63, 2005.

[52] Xunhe, Yin, Yong, Ren and Xiuming, Shan "Synchronization of discrete spatiotemporal chaos by using variable structure control", Chaos, Solitons & Fractals Vol. 14;1077-1082, 2002.

[53] Wang Chun-Chieh and Su Juhng-Perng "A novel variable structure control

scheme for chaotic synchronization", Chaos, Solitons & Fractals Vol. 2;275-287, 2003.

[54] Bai E.-W., Lonngren K.-E. "Sequential synchronization of two Lorenz systems using active control", Chaos, Solitons & Fractals 7;1041-44, 2000.

[55] Li Z., Han C.-Z. and Shi S.-J. "Modification for synchronization of Rossler and Chen chaotic systems", Phys Lett A 3-4; 224-30, 2002.

[56] Ho M.-C., Hung Y.-C. and Chou C.H. "Phase and anti-phase synchronization of two chaotic systems by using active control", Phys Lett A 1; 43-48, 2002.

[57] Yassen M.-T. "Chaos synchronization between two different chaotic systems using active control", Chaos, Solitons & Fractals Vol. 23;153-158, 2005.

[58] Agiza H.-N. and Yassen M.-T. "Synchronization of Rossler and Chen chaotic dynamical systems using active control", Phys Lett A 278;191-197,2001.

[59] Chen H.-K. and Lee C.-I "Anti-control of chaos in rigid body motion", Chaos, Solitons and Fractals Vol. 21; 957-965, 2004.

[60] Ge Z.-M. and Wu H.-W. "Chaos synchronization and chaos anticontrol of a suspended track with moving loads", Journal of Sound and Vibration Vol. 270; 685-712, 2004.

[61] Ge Z.-M., Yu C.-Y. and Chen Y.-S. "Chaos synchronization and chaos anticontrol of a rotational supported simple pendulum", JSME International Journal, Series C, Vol. 47; No. 1, 233-41, 2004.

[62] Ge Z.-M. and Leu W.-Y. "Anti-control of chaos of two-degree-of-freedom louderspeaker system and chaos system of different order system", Chaos, Solitons and Fractals Vol. 20; 503-21, 2004.

[63] Ge Z.-M., Cheng J.-W. and Chen Y.-S. "Chaos anticontrol and synchronization of three time scales brushless DC motor system", Chaos, Solitons and Fractals Vol. 22; 1165-82, 2004.

[64] Chen H.-K. “Global chaos synchronization of new chaotic systems via nonlinear control”, Chaos, Solitons & Fractals 4; 1245-51, 2005.

[65] Park Ju-H. “Chaos synchronization of a chaotic system via nonlinear control”, Chaos, Solitons & Fractals Vol.23;153-158, 2005.

[66] Huang L.-L., Feng R.-P. and Wang M. “Synchronization of chaotic systems via nonlinear control”, Phys Lett A 4 271-75, 2004.

[67] Shahverdiev, E.M., Sivaprakasam, S., and Shore, K.A. “Lag synchronization in time-delayed systems”, Phys Lett A 292;320-324, 2002.

[68] Li Guo-Hui and Zhou Shi-Ping “An observer-based anti-synchronization”, Chaos, Solitons and Fractals Vol. 29; 495-498, 2006.

[69] Hale JK, Lunel SMV. “Introduction to functional differential equations”. New York: Springer; 1993.

[70] Fischer I, Liu Y, Davis P. “Synchronization of chaotic semiconductor laser dynamics on subnanosecond time scales and its potential for chaos communication”. Phys Rev A 2000;62:011801(R).

[71] K. B. Oldham and J. Spanier, “The Fractional Calculus . San Diego, CA: Academic”, 1974.

[72] A. Charef, H. H. Sun, Y. Y. Tsao, and B. Onaral, “Fractal system as represented by singularity function,” IEEE Trans. Automat. Contr., vol. 37, pp. 1465-1470, Sept. 1992.

[73] Hartley, T.T., Lorenzo, C.F. and Qammer, H.K., “Chaos in a fractional order Chua’s system”, IEEE Trans CAS-I 1995;42:485–90.

[74] Khanin YaI. Chaos 1996;6:373.

[75] Arecchi FT, Giacomelli G, Lapucci A, Meucci R. Phys Rev A 1994;43:4997.

[76] Voss HU. Phys Rev E 2000;61:5115.

[77] Masoller C, Zanette DH. Physica A 2001;300:359.

[78] Shahverdiev EM, Sivaprakasam S, Shore KA. SPIE Proc: Phys Simulat Optoelectron Dev 2002;4646:653.

[79] Shahverdiev EM, Sivaprakasam S, Shore KA. Phys Rev E 2002;66:017204.

# Appendix

Table 1. FRACTIONAL OPERATORS WITH APPROXIMATELY 2 db ERROR FROM $\omega$ = $10^{-2}$ TO $10^{2}$ rad/sec

| |
|---|
| $\frac{1}{s^{0.1}} \approx \frac{220.4s^4 + 5004s^3 + 503s^2 + 234.5s + 0.484}{s^5 + 359.8s^4 + 5742s^3 + 4247s^2 + 147.7s + 0.2099}$ |
| $\frac{1}{s^{0.2}} \approx \frac{60.95s^4 + 816.9s^3 + 582.8s^2 + 23.24s + 0.04934}{s^5 + 134s^4 + 956.5s^3 + 383.5s^2 + 8.953s + 0.01821}$ |
| $\frac{1}{s^{0.3}} \approx \frac{23.76s^4 + 224.9s^3 + 129.1s^2 + 4.733s + 0.01052}{s^5 + 64.51s^4 + 252.2s^3 + 63.61s^2 + 1.104s + 0.002267}$ |
| $\frac{1}{s^{0.4}} \approx \frac{25s^4 + 558.5s^3 + 664.2s^2 + 44.15s + 0.1562}{s^5 + 125.6s^4 + 840.6s^3 + 317.2s^2 + 7.428s + 0.02343}$ |
| $\frac{1}{s^{0.5}} \approx \frac{15.97s^4 + 593.2s^3 + 1080s^2 + 135.4s + 1}{s^5 + 134.3s^4 + 1072s^3 + 543.4s^2 + 20.1s + 0.1259}$ |
| $\frac{1}{s^{0.6}} \approx \frac{8.579s^4 + 255.6s^3 + 405.3s^2 + 35.93s + 0.1696}{s^5 + 94.22s^4 + 472.9s^3 + 134.8s^2 + 2.639s + 0.009882}$ |
| $\frac{1}{s^{0.7}} \approx \frac{4.406s^4 + 177.6s^3 + 209.6s^2 + 9.179s + 0.0145}{s^5 + 88.12s^4 + 279.2s^3 + 33.3s^2 + 1.927s + 0.0002276}$ |
| $\frac{1}{s^{0.8}} \approx \frac{5.235s^3 + 1453s^2 + 5306s + 254.9}{s^4 + 658.1s^3 + 5700s^2 + 658.2s + 1}$ |
| $\frac{1}{s^{0.9}} \approx \frac{1.766s^2 + 38.27s + 4.914}{s^3 + 36.15s^2 + 7.789s + 0.01}$ |